THE ASTROPHYSICAL JOURNAL SUPPLEMENT SERIES, 34:425–450, 1977 August

ON THE INTEGRATION OF THE BBGKY EQUATIONS FOR THE DEVELOPMENT OF STRONGLY NONLINEAR CLUSTERING IN AN EXPANDING UNIVERSE*

MARC DAVIS†
Center for Astrophysics, Harvard College Observatory and Smithsonian Astrophysical Observatory
AND
P. J. E. PEEBLES
Joseph Henry Laboratories, Physics Department, Princeton University
Received 1976 October 11

ABSTRACT

This paper deals with the question of whether the observed galaxy correlation functions could have evolved out of "reasonable" initial conditions in the early universe. The evolution of density correlations in an expanding universe can be described by the BBGKY equations. This approach has been the subject of several previous studies, but always under the assumption of small-amplitude fluctuations, where the hierarchy of equations has a natural truncation (one ignores the reduced three-point correlation function). Results of these studies cannot be compared to the present universe because the galaxy two-point correlation function $\xi(r)$ is much greater than unity at $r \leqslant 1\ h^{-1}$ Mpc, and the three-point function ζ is on the order of $\xi(r)^2$. In this strongly nonlinear situation the hierarchy is dominated by terms ignored in the linear analysis. Our method of truncating the hierarchy is based on the empirical result that ζ can be represented to good accuracy as a simple function of ξ. We solve the equations via the velocity-moment method, and we truncate the resulting velocity-moment hierarchy for the two-point function by assuming that the distribution in the relative velocity of particle pairs has zero skewness about the mean. The second equation in this velocity-moment hierarchy is our main equation for ξ. It involves the three-point spatial correlation function ζ, which we write as a function of ξ following the empirical result. The third equation involves the first velocity moment of the three-point position and velocity correlation function. We model this term in a way consistent with our model for ζ and with a constraint equation that expresses conservation of triplets.

The equations admit a similarity transformation if (1) the effects of the discreteness of particles can be ignored, (2) the initial spectrum of density perturbations assumes a power law shape, and (3) the universe is described by an Einstein–de Sitter model ($\Omega \approx 1$). The numerical results presented here are based on this similarity solution.

The main results are the shape of $\xi(r)$ and the value of the dimensionless coupling parameter Q in ζ (eq. [4]). The computed Q is in good agreement with the observations. The prospects for testing the computed details in the shape of ξ are discussed elsewhere (Davis, Groth, and Peebles 1977). Auxiliary functions in the computation are the mean and mean-square values of $\boldsymbol{v}_{21}$, the relative peculiar velocity of particle pairs at separation x. The transverse and radial parts of $\langle v_{21}{}^{\alpha} v_{21}{}^{\beta} \rangle$ at small x are close to isotropy, suggesting that clusters, once formed, leave little trace of radial infall. Also, $\langle v_{21}{}^{\alpha} \rangle$ gives no evidence of "overshoot" or collapse of protoclusters. These results suggest that the velocity dispersion within a protocluster grows as it is developing as a density perturbation, so that when the cluster fragments out of the general expansion it is already "virialized."

Subject headings: cosmology — functions: numerical methods — galaxies: clusters of

I. INTRODUCTION

This paper is the first in a projected series on an attempt to numerically integrate the BBGKY equations describing the evolution of the galaxy correlation functions in an expanding universe. The goal is to discover those conditions (if any) under which the predicted functions would match the observations (Peebles 1974; Peebles and Groth 1975; Groth and Peebles 1977). The point of attack described here takes from the theory of nonideal gases the BBGKY equations for the n-point correlation functions in position and velocity (see, e.g., Montgomery and Tidman 1964). The attractive feature of this approach is that the theory deals with functions quite close to those that have been directly estimated from the data. The problem is that the theory yields an infinite set of

* Research supported in part by the National Science Foundation.
† Alfred P. Sloan Fellow.

coupled equations involving all orders of the correlation functions. For plasmas, the standard approach is to use a "weak coupling" hypothesis which assumes that the particle correlations are progressively less important the higher the order, so that the hierarchy may be truncated by dropping the (reduced) correlation functions beyond some chosen order. This is appropriate for a stable plasma but not for a strongly turbulent plasma (Ichimaru 1973). For the galaxy distribution, we know that on scales $r \leqslant 1$ Mpc the reduced three-point spatial correlation function ζ is on the order of $\zeta^2 \gg \xi \gg 1$, where $\xi(r)$ is the two-point function, and the four-point function Υ is on the order of $\xi^3 \gg \zeta$. At least to this order the reduced correlation functions increase going up the hierarchy, just contrary to what is assumed for a stable plasma. The basis of our approach is the empirical result that, to remarkable accuracy, ζ can be represented as a simple function of ξ. We use this together with a consistency constraint (the law of "conservation of triplets," eq. [49] below) to guess at a form for the three-point spatial and velocity function in terms of the two-point function. This closes the BBGKY hierarchy, leaving us with a nonlinear integrodifferential equation which, with further approximations, we simplify to the point where numerical solution is practical.

The BBGKY equations have figured in a number of discussions of the evolution of irregularities in an expanding universe. The first approaches were directed to a Vlasov equation, where one considers a single-particle distribution function in a potential field given in a self-consistent way by the smoothed-out particle distribution (van Albada 1960; Gilbert 1966; Bisnovatyi-Kogan and Zel'dovich 1971; Saslaw 1972). This is reasonable for a rich cluster of galaxies, but it is questionable whether the notion of a single-particle distribution function is useful for describing the general complex of groups and clusters. Gilbert (1965), Saslaw (1972), Fall and Saslaw (1976), Fall and Severne (1976), Inagaki (1976), and Yahil (1976) all have discussed properties of the cosmological BBGKY equations under the "weak coupling" approximation that the reduced third-order correlation function is negligible. This may be relevant at an epoch when the "particles"—perhaps hydrogen atoms, perhaps discrete galaxies—are nearly uniformly distributed. (Even under the assumption of the gravitational instability picture, it is not guaranteed that such an epoch exists, for it may be that the clustering always is strongly nonlinear on small enough scales.) None of these studies is adapted to the specific problem of describing the development of strongly nonlinear clustering in the gravitational instability picture. Because galaxies are strongly clustered, the universe must be considered as a strongly nonideal gas. Our goal in this paper is to find an approach that deals with the central features, though necessarily not all the details, of this problem.

In the next section we list the main concepts and approximations that are employed, and we outline the main steps in the calculation.

II. BASIC ASSUMPTIONS AND APPROXIMATIONS

a) The Cosmological Model and the Description of the Matter Distribution

We use the standard Friedman-Lemaître model with $\Lambda = 0$. Radiation is ignored. Matter is described as a collection of pointlike particles (perhaps hydrogen atoms, or, for some purposes, individual galaxies), each of mass m. The particles interact only through gravity as described in the linear, nonrelativistic, approximation—that is, Newtonian mechanics (cf. Peebles 1971*a*, pp. 213–217). We use spatial coordinates x^α expanding with the background cosmological model, so a locally Minkowskian coordinate system is defined by

$$r^\alpha = a(t)x^\alpha \,, \tag{1}$$

where $a(t)$ is the expansion parameter. The time variable t is proper cosmic time in the background model.

The particle distribution is taken to be a homogeneous and isotropic random process. Thus we imagine a statistical ensemble of universes with correlation functions defined by averages across the ensemble. Because we treat the perturbation to the geometry in the linear approximation for g_{ij}, we can define a member of the ensemble by a list of coordinate $x_i^\alpha(t)$, $p_i^\alpha(t)$ for all the particles that happen to be in that universe. The goal is to compute the time evolution of the particle correlation functions under these assumptions. Of course it is a matter for separate discussion to decide whether the observation of the galaxy correlations yields useful measures of these mass correlation functions.

b) Model for the Three-Point Function

The central basis for the calculation is the assumption that the three-point position and velocity correlation function may be modeled in terms of the two-point function. The evidence for this assumption and its meaning are discussed here.

The two-point spatial correlation function $\xi(r)$ may be defined through the probability of finding a particle in the volume element dV at distance r from a particle randomly chosen from the ensemble,

$$dP \equiv n[1 + \xi(r)]dV \,. \tag{2}$$

Here n is the mean particle number density. The three-point spatial correlation function ζ may be defined through the joint probability of finding a particle in each of the volume elements dV_1, dV_2 that, with a particle randomly chosen from the ensemble, define a triangle with sides r_a, r_b, r_c:

$$dP \equiv n^2(1 + \xi_a + \xi_b + \xi_c + \zeta_{abc})dV_1 dV_2 , \tag{3}$$

where the subscripts represent the arguments. The data from the Zwicky and Shane-Wirtanen catalogs are in good agreement with the models:

$$\begin{aligned} &\xi(r) \approx (r_c/r)^{1.8} , \quad r_c \approx 5\, h^{-1}\,\text{Mpc} , \quad r \leqslant r_c ; \\ &\zeta_{abc} = Q(\xi_a\xi_b + \xi_b\xi_c + \xi_c\xi_a) , \\ &Q \approx 0.85 \quad \text{(Zwicky)} , \\ &Q \approx 1.24 \quad \text{(Shane-Wirtanen)} \end{aligned} \tag{4}$$

(Peebles and Groth 1975; Groth and Peebles 1977). The reliable estimates of ξ and ζ are in the range of separations $\sim 100\, h^{-1}$ kpc to $\sim 10\, h^{-1}$ Mpc ($h \equiv$ Hubble's constant in units of 100 km s^{-1} Mpc^{-1}), where $\xi \gtrsim 1$.

Equation (4) for ζ with $Q = 1$ resembles the Kirkwood superposition approximation occasionally used in liquid physics and turbulence theory, except that the term $\xi_a\xi_b\xi_c$ is missing (Ichimaru 1973, p. 272; Totsuji and Ichimaru 1974; Rice and Gray 1975). If this term were present with coefficient close to unity it would have dominated the observations, since $\xi \gtrsim 1$, making the variation of the angular three-point function with θ very different from what is observed. Thus we believe that the Kirkwood superposition approximation is not relevant here.

A model that does seem to be useful is the continuous clustering hierarchy. This can be stated as follows. Suppose the matter distribution is observed with resolution r, that is, after smoothing by a running average of width r, where $r \leqslant 10\, h^{-1}$ Mpc [so $\xi(x) \gtrsim 1$]. It is assumed that the matter thus smoothed would appear in clumps, the clumps having typical size r, and the typical density within a clump being $N(r)$. Then $N(r) \approx n[1 + \xi(r)] \approx n\xi(r)$ (for $\xi \gtrsim 1$). To see this, suppose a particle is chosen at random and dV placed at distance r. Then the particle and dV tend to be in the same clump of size $\sim r$, so the mean density at dV is $\sim N(r)$. Similarly, if a particle is chosen at random and dV_a and dV_b placed at distances r_a and r_b, then the probability of finding a particle in dV_a is $\sim N(r_a)dV_a$, because the chosen particle and dV_a tend to be in the same clump of size r_a, and the probability of finding a particle in dV_b is $\sim N(r_b)dV_b$. Thus the joint probability for finding particles in both elements is $\sim N(r_a)N(r_b)dV_a dV_b$. This is in general agreement with equations (3) and (4) in predicting (a) that if the triangle shape is held fixed ζ scales with the triangle size r as $r^{-2\gamma}$, and (b) that if the small side of the triangle is held fixed at r then ζ varies with the size r_l of the large side roughly as $r_l^{-\gamma}$.

Since ξ measures the mean density at distance x from a particle, and ζ measures the mean square density, the parameter Q in equation (4) measures the dispersion of the density in the clumps at characteristic size r. More generally, the number N_n of particles found within distance r of a randomly chosen particle satisfies (Peebles 1975)

$$\begin{aligned} \langle N_n \rangle &= nV + n\int \xi d^3r , \\ \langle (N_n - \langle N_n \rangle)^2 \rangle &= \langle N_n \rangle + n^2 \int d^3r_1 d^3r_2 \xi(r_{12}) + (Q - 1)n^2\left[\int \xi(r)d^3r\right]^2 + 2Qn^2 \int d^3r_1 d^3r_2 \xi(r_1)\xi(r_{12}) \\ &\approx (3Q - 1)(nV)^2\xi(r)^2 , \quad V = 4\pi r^3/3 , \end{aligned}$$

where the integrals are over the sphere of radius r and the last line follows if $\xi \propto r^{-\gamma}$, $\gamma < 3$, and $\xi(r) \gg 1$. Thus Q cannot be less than about 0.3, and Q measures the dispersion in the number of neighbors. One therefore expects that, in the hierarchical clustering picture, Q ought to be on the order of unity, but of course this leaves considerable latitude in its actual value.

c) Velocity Moments and the Stability Assumption

To reduce the number of independent variables we take velocity moments of the second-order BBGKY equation (and of course we assume they exist). The relevant velocity here is the relative peculiar velocity of a particle pair at separation x. To truncate the resulting hierarchy of velocity moments, we assume that the velocity distribution has zero skewness about the mean (see § VI). In stellar dynamics zero skewness means that there is no kinetic energy flux as measured by an observer moving with the mean streaming velocity, and it is known that, in stellar dynamics, nonzero skewness is needed to describe relaxation processes (see, e.g., van Albada 1960; Henon 1961; Lynden-Bell and Wood 1968; Larson 1970). The meaning of the velocity distribution is different here, but we might expect that similar objections apply to the zero skewness assumption. This is not necessarily a problem, because the formation of protoclusters may not be appreciably affected by kinetic energy flux into or out of the protosystem. The more serious question is whether the clusters, once formed and "virialized," continue to evolve through relaxation processes. One suspects that dissipation has very substantially affected the pattern of the mass distribution on the scale of galaxy sizes and smaller. It is hard to judge whether two-body relaxation has been important in the scales where ξ and ζ are observed, $r \gtrsim 100\, h^{-1}$ kpc, for we do not have a clear picture for the typical effective number of particles (coherent mass lumps) within a cluster on a given scale. We will be assuming that the clustering hierarchy, once formed and in dynamic equilibrium, has negligible subsequent evolution.

d) *Initial Conditions*

In the gravitational instability picture the nature of the presently observed clumping of matter, in galaxies, clusters, and so on, is determined by the character of the assumed growing density fluctuations in the early universe. We assume that these density perturbations can be approximated as a random Gaussian (random phase) process with power spectrum

$$\langle|\delta_k|^2\rangle \propto k^n\,, \tag{5}$$

where k is the wave number and n is a constant (Peebles 1965). This is supposed to apply at any epoch t (subsequent to decoupling of matter and radiation) and at $k \lesssim 2\pi/\lambda_m(t)$, where $\lambda_m(t)$ is the wavelength at which $\delta\rho/\rho \geq 1$. The character of the initial conditions thus is completely determined by two numbers, λ_m at some starting time t_i and the index n. This has the advantage of simplicity. Of course the test will be to discover how broad a range of phenomena can be successfully predicted from the assumption.

The two-point correlation function is the Fourier transform of the power spectrum. For large x, where the relevant part of the spectrum is the "primeval" shape given by equation (5), this gives

$$\xi(x) = Bx^{-(3+n)}D(t)^2\,, \tag{6}$$

$$D^2 \propto t^{4/3} \qquad \text{if} \qquad \Omega = 1\,,$$

where $B > 0$ if $-3 < n < 0$ or $2 < n < 4$ and $B < 0$ if $0 < n < 2$ (Peebles and Groth 1976). The time dependence factor $D^2(t)$ depends on the cosmological model. For the Einstein–de Sitter model and a pure growing density perturbation, $D^2 \propto t^{4/3}$, as indicated. Scaling arguments plus the stability assumption of § II*c* say that v at small x varies as (Peebles 1965, 1974; § IX below).

$$\xi \propto x^{-\gamma}\,, \qquad \gamma = (9 + 3n)/(5 + n)\,. \tag{7}$$

The observed two-point correlation function at small x indicates that $\gamma \approx 1.8$, and thus $n \approx 0$. The theory developed here applies when $-1 < n < 1$, but the numerical method is not adapted to the special case $n = 0$. We approach this special case by taking n small but nonzero. Since the character of the observable part of the solutions does not change discontinuously at $n = 0$, this should cause no problem. The goal of the present calculation is to see how $\xi(x)$ makes the transition between the known asymptotic behavior at large and small x as given by equations (6) and (7).

e) *Scaling Behavior*

The existence of a similarity (scaling) solution to the BBGKY equations depends on two assumptions, that the expansion of the universe approximate the Einstein–de Sitter model ($\Lambda = p = 0$, $\Omega = 1$), so it presents no characteristic lengths or times; and that the matter interaction presents no characteristic lengths. The similarity solution applies if the initial conditions are suitably chosen, as described in this section.

Scale invariance of the matter interaction means that (1) nongravitational forces are negligible, and (2) the length $n^{-1/3}$, where n is the mean particle density, is negligibly small (see § III*g*). The first assumption is not valid on scales less than the size of a galaxy, where gas dynamics is thought to have been important, but this should not affect the evolution of structure on scales of interest, $r \gtrsim 100\, h^{-1}$ kpc. That is, in the computation we assume that the matter clustering satisfies a universal scaling behavior down to arbitrarily small lengths, and we argue that the results may be a reasonable approximation for length scales of interest, even though they are not valid on small scale. The second point couples to the first: if the "fundamental particles" m were giant pointlike galaxies, then $n^{-1/3}$ would be on the order of $5\, h^{-1}$ Mpc, and the scaling solution could be valid only at very large separations. On the other hand, if one assumed that galaxies and clusters of galaxies evolved out of small-scale initial irregularities according to the same physical process operating on different scales, with gas dynamics subsequently removing the subclustering on scales $\lesssim 10\, h^{-1}$ kpc, then, as argued for the first point, the similarity solution may well be valid at $r \gtrsim 100\, h^{-1}$ kpc.

In a similarity solution the initial conditions are fixed: the power spectrum at $k < 2\pi/\lambda_m$ must be a pure power law, for otherwise it would present a characteristic length, and δ_k at $k < 2\pi/\lambda_m$ must be evolving like a pure growing density perturbation. (As discussed in § XI, other similarity solutions involving the decaying mode exist but are not acceptable because ξ diverges at infinite spatial separation.) This latter condition could not apply just after decoupling (redshift $z \approx 1000$) because the radiation drag has substantially affected the matter velocity, but it may be that by $z \approx 100$ the decaying mode has become small compared to the growing mode. If so, and if the power spectrum agrees with equation (5), then the boundary conditions agree with the similarity solution.

Scaling greatly simplifies the numerical problem because it eliminates the time variable, replacing $\boldsymbol{x}$ with $\boldsymbol{s} \propto \boldsymbol{x}/t^{\alpha}$, with α a constant (§ IX below). In an open or closed cosmological model scaling is not valid when Ω is substantially different from unity, but the similarity solution still is important because it applies in the early universe, where the universe expands as if it were cosmologically flat. The similarity solution thus can be used to fix initial conditions for the integration forward in time.

f) Plan of Attack

In § III we derive the first three BBGKY equations. The first two of these have been derived in somewhat different forms in the references cited above, but it seems useful to repeat the derivations using concepts and conventions more closely adapted to the present problem. In § IV we obtain velocity moments of these BBGKY equations. The central equation for the calculation is the first moment of the second BBGKY equations, which reduces to a differential equation for $\xi(x, t)$ (eq. [50c]). This equation has two "difficult" terms, an integral over ζ and the second moment of the relative peculiar velocity (eq. [50c] below). We deal with the first term by using equation (4). To get at the second term we go to the second velocity moment of the second BBGKY equation (eq. [50d]). This introduces the third velocity moment of the two-point correlation function. In § VI we reduce this third moment under the assumption of zero skewness. It also introduces the first velocity moment of the three-point position and velocity correlation function d. In § VII we arrive at an assumed form for d (eq. [62]) guided by equation (4) for the spatial part and an equation expressing conservation of triplets (eq. [50e]). This leaves a closed set of equations in two variables, x and t (eqs. [71], [72], [76], and [79]). Application of the scaling transformation to reduce to one independent variable is described in § IX.

Even with the scaling assumption the numerical problem is formidable, so in § X we introduce approximate expressions to simplify some multidimensional integrals (eqs. [73] and [75]). The expressions are accurate at small x, where they play an important role, but are only approximate in the "transition region" where $\xi \approx 1$. This approach is not unreasonable because the empirical basis for our modeling of the three-point function d is accurate at $\xi \gg 1$, rather weak at $\xi \approx 1$, and nonexistent at $\xi \ll 1$. The last part is unimportant because when $\xi \ll 1$ we can assume that d is negligible compared to other terms in the equation for ξ. The treatment of the transition region necessarily is uncertain because of the problem with d, and the best we can do is to ask how sensitive the final results are to the approximations used in treating the transition. As described in § XIII, the results are not very sensitive to the treatment of the three-point function.

In § XI we derive asymptotic solutions to the equations in the limiting cases of small separation and large separation. The initial condition (eq. [5]) is applied via the selection of the wanted asymptotic solutions. As discussed in § XI*c*, joining these solutions gives rise to an eigenvalue problem, which serves to fix Q (eq. [4]). The method of integration is described in § XII, the results are presented in § XIII, and the possible implications of the results are considered in § XIV.

III. DERIVATION OF THE BBGKY EQUATIONS

a) The Equations of Motion

A Lagrangian for the path $x^{\alpha}(t)$ of one particle moving in the field of the others is, under the assumptions in § IIa,

$$\mathscr{L} = \tfrac{1}{2}ma^2\left(\frac{d\boldsymbol{x}}{dt}\right)^2 - m\phi\,, \tag{8}$$

giving the canonical momentum

$$p^{\alpha} = ma^2\frac{dx^{\alpha}}{dt}\,, \tag{9}$$

which is related to the proper peculiar velocity v^{α} (proper velocity relative to the background cosmological model) by

$$p^{\alpha} = mav^{\alpha}\,. \tag{10}$$

The equations of motion are

$$\frac{dp^{\alpha}}{dt} = -m\frac{\partial\phi}{\partial x^{\alpha}}\,. \tag{11}$$

The field equation for the potential ϕ is

$$\nabla^2\phi = 4\pi Ga^2[\rho(\boldsymbol{x}, t) - \langle\rho(t)\rangle]\,, \tag{12}$$

where $\langle\rho\rangle$ is the density in the background cosmological model. The Green's function solution to equation (12), differentiated to get the force, is

$$-\frac{\partial\phi}{\partial x^\alpha} = Ga^2 \int [\rho(\boldsymbol{x}') - \langle\rho\rangle] \frac{x'^\alpha - x^\alpha}{|\boldsymbol{x}' - \boldsymbol{x}|^3} d^3x' . \tag{13}$$

This integral is well behaved at large $|\boldsymbol{x}' - \boldsymbol{x}|$ because $\rho - \langle\rho\rangle$ fluctuates around zero. We can write it as the difference of integrals over ρ and $\langle\rho\rangle$ if we adopt the convention that one integrates first over angles at fixed $|\boldsymbol{x}' - \boldsymbol{x}|$, then over $|\boldsymbol{x}' - \boldsymbol{x}|$. In the point particle picture, ρ is a sum of terms like $ma^{-3}\delta[\boldsymbol{x} - \boldsymbol{x}_i(t)]$, and equation (13) becomes

$$-\frac{\partial\phi}{\partial x^\alpha} = \frac{Gm}{a} \sum_j \frac{x_j{}^\alpha - x^\alpha}{|\boldsymbol{x}_j - \boldsymbol{x}|^3}, \tag{14}$$

with the prescription that the sum is ordered by increasing $|\boldsymbol{x}_j - \boldsymbol{x}|$ and that

$$\int d^3x' \frac{(x'^\alpha - x^\alpha)}{|\boldsymbol{x}' - \boldsymbol{x}|^3} = 0 . \tag{15}$$

The equation of motion for the ith particle is then (eqs. [11] and [14])

$$\frac{dp_i{}^\alpha}{dt} = \frac{Gm^2}{a} \sum_{j \neq 1} \frac{x_j{}^\alpha - x_i{}^\alpha}{|\boldsymbol{x}_j - \boldsymbol{x}_i|^3}, \tag{16}$$

where the right side is the ordered sum over all particles other than i.

b) Definitions of the n-Point Correlation Functions

The one-point distribution function gives the probability of finding a particle in the small volume element d^3x and moving with momentum $\boldsymbol{p}$ within the small range d^3p,

$$dP = \rho_1(\boldsymbol{p}, t)d^3xd^3p . \tag{17}$$

The assumptions of homogeneity and isotropy say that ρ_1 depends only on the magnitude of $\boldsymbol{p}$. The normalization condition is

$$\int \rho_1 d^3p = na^3 = \text{constant} , \tag{18}$$

where na^3 is the particle number density in $\boldsymbol{x}$ coordinates.

The two-point function gives the joint probability of finding a particle in d^3x_1 moving with momentum $\boldsymbol{p}_1$ in the range d^3p_1, and of finding a second particle at $\boldsymbol{x}_2, \boldsymbol{p}_2$ in d^3x_2, d^3p_2:

$$dP = \rho_2(1, 2)d^3x_1d^3p_1d^3x_2d^3p_2 . \tag{19}$$

The reduced two-point correlation function c is defined by the equation

$$\rho_2(1, 2) = \rho_1(1)\rho_1(2) + c(1, 2) . \tag{20}$$

The first term is the distribution expected if the particles were uncorrelated. The term c integrated over momenta gives the spatial correlation function (eq. [2]),

$$\int d^3p_1d^3p_2c(1, 2) = n^2a^6\xi(|\boldsymbol{x}_2 - \boldsymbol{x}_1|, t) . \tag{21}$$

The three-point correlation function $\rho_3(1, 2, 3)$ is defined in exact analogy to equation (19). The reduced three-point function d is defined by

$$\rho_3(1, 2, 3) = \rho_1(1)\rho_1(2)\rho_1(3) + \rho_1(1)c(2, 3) + \rho_1(2)c(3, 1) + \rho_1(3)c(1, 2) + d(1, 2, 3) . \tag{22}$$

On integrating ρ_3 over all momenta one finds

$$\int dd^9p = n^3a^9\zeta(1, 2, 3) , \tag{23}$$

with ζ the spatial correlation function (eq. [3]).

c) The BBGKY Equations

The standard derivation of the BBGKY equations for the ρ_n starts from an imagined fixed number of particles confined to a box (see, e.g., Montgomery and Tidman 1964). For the cosmological problem it seems more direct to proceed in another way. Isolate a small (in the limit, infinitesimal) patch of space around $\boldsymbol{x}_1$ and a small range of momenta around $\boldsymbol{p}_1$. The positions $\boldsymbol{x}_i$ of all the other particles in the universe at fixed time t can be specified as some configuration $\mathscr{H}$. Next, select from the ensemble of universes those with a particular configuration $\mathscr{H}$. In this subensemble the probability of finding a particle in the infinitesimal element $d^3x_1d^3p_1$ in the patch is written as

$$dP = \rho_1(\boldsymbol{x}_1, \boldsymbol{p}_1, t|\mathscr{H})d^3x_1d^3p_1 \,. \tag{24}$$

A particle found in the patch is moving in a definite way under its interaction with all the rest of the matter as specified by $\mathscr{H}$ (we can assume that the probability that there are two particles in the patch is negligible compared to the probability that there is one). By Liouville's theorem (with eq. [9]),

$$\left(\frac{\partial}{\partial t} + \frac{p_1{}^\alpha}{ma^2}\frac{\partial}{\partial x_1{}^\alpha} + \frac{dp_1{}^\alpha}{dt}\frac{\partial}{\partial p_1{}^\alpha}\right)\rho_1(\boldsymbol{x}_1, \boldsymbol{p}_1, t|\mathscr{H}) = 0 \,. \tag{25}$$

This expression may be averaged across the configurations. We have

$$\begin{aligned} \langle\rho_1(\boldsymbol{x}_1, \boldsymbol{p}_1, t|\mathscr{H})\rangle_{\mathscr{H}} &\equiv \rho_1(\boldsymbol{p}_1, t)\,, \\ \langle\partial\rho_1/\partial x_1{}^\alpha\rangle_{\mathscr{H}} &= \partial\rho_1(\boldsymbol{p}_1, t)/\partial x_1{}^\alpha = 0\,, \\ \langle\partial\rho_1/\partial t\rangle_{\mathscr{H}} &= \partial\rho_1(\boldsymbol{p}_1, t)/\partial t\,, \end{aligned} \tag{26}$$

where the last line follows because $\mathscr{H}$ is specified at fixed time t. The last term in equation (25) is

$$\left\langle\frac{dp_1{}^\alpha}{dt}\frac{\partial\rho_1}{\partial p_1{}^\alpha}\right\rangle_{\mathscr{H}} = \frac{\partial}{\partial p_1{}^\alpha}\left\langle\rho_1(1|\mathscr{H})\frac{dp_1{}^\alpha}{dt}\right\rangle_{\mathscr{H}} = \frac{Gm^2}{a}\frac{\partial}{\partial p_1{}^\alpha}\int d^3x_2d^3p_2\frac{x_{21}{}^\alpha}{x_{21}{}^3}\rho_2(1, 2)\,,$$
$$x_{21}{}^\alpha = x_2{}^\alpha - x_1{}^\alpha\,, \qquad |\boldsymbol{x}_{21}| = x_{21}\,, \tag{27}$$

where we have used equations (16) and (19). On replacing ρ_2 with c (eq. [20]), and using equation (15), we arrive at the first BBGKY equation,

$$\frac{\partial\rho_1(\boldsymbol{p}_1, t)}{\partial t} + \frac{Gm^2}{a}\frac{\partial}{\partial p_1{}^\alpha}\int d^3x_2d^3p_2c(1, 2)\frac{x_{21}{}^\alpha}{x_{21}{}^3} = 0\,. \tag{28}$$

This is equivalent to Fall and Severne's (1976) equation (2.6).

In a similar way we can isolate two small patches around $\boldsymbol{x}_1, \boldsymbol{p}_1$ and $\boldsymbol{x}_2, \boldsymbol{p}_2$, label the positions $\boldsymbol{x}_i$ of all the other particles in the universe by the configuration $\mathscr{H}'$, and for the subensemble of universes with configuration $\mathscr{H}'$ write the joint probability of finding particles in each of two infinitesimal elements, one in each patch, as

$$dP = \rho_2(1, 2, t|\mathscr{H}')d^3x_1d^3x_2d^3p_1d^3p_2\,. \tag{29}$$

Particles in 1 and 2 are moving in a definite way under the interaction with each other and with the rest of the universe. This is described by the Liouville equation

$$\left(\frac{\partial}{\partial t} + \frac{p_1{}^\alpha}{ma^2}\frac{\partial}{\partial x_1{}^\alpha} + \frac{p_2{}^\alpha}{ma^2}\frac{\partial}{\partial x_2{}^\alpha} + \frac{dp_1{}^\alpha}{dt}\frac{\partial}{\partial p_1{}^\alpha} + \frac{dp_2{}^\alpha}{dt}\frac{\partial}{\partial p_2{}^\alpha}\right)\rho_2(1, 2|\mathscr{H}') = 0\,. \tag{30}$$

On averaging this across $\mathscr{H}'$, using ρ_3 to evaluate $\langle\rho_2(1, 2|\mathscr{H}')dp_1{}^\alpha/dt\rangle$, and following the arguments that lead to equation (28), one finds

$$\begin{aligned} &\frac{\partial}{\partial t}\rho_2(1, 2) + \frac{p_1{}^\alpha}{ma^2}\frac{\partial}{\partial x_1{}^\alpha}\rho_2(1, 2) + \frac{Gm^2}{a}\frac{x_{21}{}^\alpha}{|x_{21}|^3}\frac{\partial}{\partial p_1{}^\alpha}\rho_2(1, 2) \\ &\qquad + \frac{Gm^2}{a}\frac{\partial}{\partial p_1{}^\alpha}\int d^3x_3d^3p_3\frac{x_{31}{}^\alpha}{x_{31}{}^3}\rho_3(1, 2, 3) + 1 \leftrightarrow 2 = 0\,. \end{aligned} \tag{31}$$

As indicated, the equation must be symmetrized by adding the result of exchanging $\boldsymbol{x}_1, \boldsymbol{p}_1 \leftrightarrow \boldsymbol{x}_2, \boldsymbol{p}_2$ in the last three terms. On using equations (20) and (22) to replace ρ_2 and ρ_3 with the reduced functions c, d, using equation (28) to eliminate the time derivative of ρ_1, and using equation (15) to eliminate the spatial integrals over ρ_1, we find the second BBGKY equation,

$$\frac{\partial}{\partial t}c(1,2) + \frac{p_1{}^\alpha}{ma^2}\frac{\partial}{\partial x_1{}^\alpha}c(1,2) + \frac{Gm^2}{a}\frac{x_{21}{}^\alpha}{x_{21}{}^3}\frac{\partial}{\partial p_1{}^\alpha}[\rho_1(1)\rho_1(2) + c(1,2)]$$
$$+ \frac{Gm^2}{a}\frac{\partial\rho_1(\boldsymbol{p}_1)}{\partial p_1{}^\alpha}\int d^3x_3d^3p_3\frac{x_{31}{}^\alpha}{|\boldsymbol{x}_{31}|^3}c(2,3) + \frac{Gm^2}{a}\frac{\partial}{\partial p_1{}^\alpha}\int d^3x_3d^3p_3\frac{x_{31}{}^\alpha}{|\boldsymbol{x}_{31}|^3}d(1,2,3)$$
$$+ 1 \leftrightarrow 2 = 0\,. \tag{32}$$

As before, the equation must be symmetrized by adding the result of interchanging coordinate labels, $\boldsymbol{x}_1, \boldsymbol{p}_1 \leftrightarrow \boldsymbol{x}_2, \boldsymbol{p}_2$ in all terms save the first. Equation (32) is equivalent to equation (2.7) of Fall and Severne (1976).

For the third BBGKY equation we have from the corresponding Liouville equation,

$$\frac{\partial}{\partial t}\rho_3(1,2,3) + \sum_{i=1,3}\left(\frac{p_i{}^\alpha}{ma^2}\frac{\partial}{\partial x_i{}^\alpha}\rho_3 + \frac{\partial}{\partial p_i{}^\alpha}F^\alpha\right) = 0\,. \tag{33}$$

Here F^α represents the sum of contributions to the rate of change of the momenta of each of the three particles. The form of F^α is lengthy and, since it is not needed here, we do not write it down.

IV. VELOCITY MOMENTS

To reduce the number of independent variables we take velocity moments, that is, we multiply each equation by a power of momentum and then integrate over all momentum arguments. This technique, standard in fluid mechanics, offers the simplest scheme of solving equation (32) while yielding only the most elementary information about the momentum dependence of $c(1, 2)$.

a) *The First BBGKY Equation*

The lowest nontrivial moment of equation (28) is the second. On multiplying the equation by $p_1{}^2$ and integrating over $\boldsymbol{p}_1$ one finds

$$\frac{d}{dt}(a^2\langle v_1{}^2\rangle) = \frac{2G}{na^4}\int p_1{}^\alpha\frac{x_{21}{}^\alpha}{|\boldsymbol{x}_{21}|^3}c(1,2)d^6pd^3x_2\,, \tag{34}$$

where equations (10) and (18) have been used to reduce the first term to the mean square value of the proper peculiar particle velocity.

b) *Pair Conservation Law*

The result of integrating equation (32) over $\boldsymbol{p}_1$ and $\boldsymbol{p}_2$ and using equation (21) is

$$n^2a^6\frac{\partial}{\partial t}\xi(x_{12},t) + \frac{\partial}{\partial x_1{}^\alpha}\int\frac{p_1{}^\alpha}{ma^2}c(1,2)d^6p + \frac{\partial}{\partial x_2{}^\alpha}\int\frac{p_2{}^\alpha}{ma^2}c(1,2)d^6p = 0\,. \tag{35}$$

This may be simplified by using the symmetry properties of c:

$$\text{homogeneity:}\quad c(1,2) = c(\boldsymbol{x}_2 - \boldsymbol{x}_1, \boldsymbol{p}_1, \boldsymbol{p}_2)\,;$$
$$\text{exchange:}\quad c(\boldsymbol{x}, \boldsymbol{p}_1, \boldsymbol{p}_2) = c(-\boldsymbol{x}, \boldsymbol{p}_2, \boldsymbol{p}_1)\,;$$
$$\text{parity:}\quad c(\boldsymbol{x}, \boldsymbol{p}_1, \boldsymbol{p}_2) = c(-\boldsymbol{x}, -\boldsymbol{p}_1, -\boldsymbol{p}_2) = c(\boldsymbol{x}, -\boldsymbol{p}_2, -\boldsymbol{p}_1)\,. \tag{36}$$

Thus, forms equivalent to equation (35) are

$$n^2a^6\frac{\partial\xi}{\partial t}(x,t) + \frac{\partial}{\partial x^\alpha}\int\frac{p_2{}^\alpha - p_1{}^\alpha}{ma^2}c(1,2)d^6p = 0\,,$$
$$n^2a^6\frac{\partial\xi}{\partial t}(x,t) - 2\frac{\partial}{\partial x^\alpha}\int\frac{p_1{}^\alpha}{ma^2}c(1,2)d^6p = 0\,, \tag{37}$$

where

$$x^\alpha \equiv x_2{}^\alpha - x_1{}^\alpha\,,\qquad x \equiv |\boldsymbol{x}|\,. \tag{38}$$

The equation is further simplified by introducing the mean relative peculiar velocity $v^\alpha = \langle v_2{}^\alpha - v_1{}^\alpha \rangle$ averaged over pairs at separation x^α. (Since $v_1{}^\alpha$ is the proper velocity of particle 1 relative to the background, the net mean proper velocity of particle 2 relative to 1 is $v^\alpha + x^\alpha da/dt$.) By symmetry, we can write

$$v^\alpha = vx^\alpha/x\,, \tag{39}$$

and by equations (19)–(21),

$$\int \frac{p_2{}^\alpha - p_1{}^\alpha}{ma} c(1, 2) d^6p = n^2a^6[1 + \xi(x, t)]v^\alpha\,. \tag{40}$$

Equations (37)–(40) give

$$\frac{\partial \xi}{\partial t} + \frac{1}{x^2 a} \frac{\partial}{\partial x} [x^2(1 + \xi)v] = 0\,. \tag{41}$$

This just expresses conservation of particle pairs. Another derivation is given by Peebles (1976*a*, eq. [16]).

It will be convenient below to use the function A defined by

$$\int (p_2{}^\alpha - p_1{}^\alpha) c(1, 2) d^6p \equiv n^2a^6 A(x, t) x^\alpha\,. \tag{42}$$

By equation (37),

$$\frac{\partial \xi}{\partial t} + \frac{1}{mx^2a^2} \frac{\partial}{\partial x} (x^3 A) = 0\,. \tag{43}$$

c) Cosmic Energy Theorem

On using

$$\frac{x_{21}{}^\alpha}{x_{21}{}^3} = -\frac{\partial}{\partial x_2{}^\alpha} \frac{1}{x_{21}}$$

in equation (34), integrating by parts, and using equation (37), we find

$$\frac{d}{dt}(a^2\langle v^2 \rangle) = \frac{2G}{na^4} \int \frac{d^3x_2}{x_{21}} \frac{\partial}{\partial x_2{}^\alpha} \int d^6p p_1{}^\alpha c(1, 2) = Gmna4 \int \frac{d^3x}{x} \frac{\partial}{\partial t} \xi(x, t)\,, \tag{44}$$

or

$$\left(\frac{d}{dt} + \frac{2}{a}\frac{da}{dt}\right) \frac{\langle v_1{}^2 \rangle}{2} = \left(\frac{d}{dt} + \frac{1}{a}\frac{da}{dt}\right) U\,,$$

$$U = \tfrac{1}{2} G\rho a^2 \int \frac{d^3x}{x} \xi(x, t)\,, \tag{45}$$

where

$$\rho = nm \tag{46}$$

is the mean mass density. Equation (45) is the Irvine (1961)–Layzer (1963) energy equation. It was independently derived from the BBGKY equations by Gilbert (1965) and by Fall and Severne (1976).

d) A Momentum Flux Equation

Next, we consider the first moment of equation (32): multiply the equation by $p_{21}{}^\beta = p_2{}^\beta - p_1{}^\beta$ and then integrate over momenta. The expression is simplified by taking the divergence $\partial/\partial x^\alpha$ and using equations (21), (23), and (37) with the identity

$$\frac{\partial}{\partial x^\alpha} \left(\frac{x^\alpha}{x^3}\right) = 4\pi \delta(\boldsymbol{x})\,.$$

The result, after some manipulation, is

$$\frac{\partial^2 \xi(x, t)}{\partial t^2} + \frac{2}{a}\frac{da}{dt}\frac{\partial \xi}{\partial t} = \frac{1}{m^2n^2a^{10}} \frac{\partial^2}{\partial x^\alpha \partial x^\beta} \int d^6p p_{21}{}^\alpha p_{21}{}^\beta c(1, 2) + \frac{8\pi Gm}{a^3} \delta(\boldsymbol{x})[1 + \xi(0)]$$

$$+ \frac{2Gm}{a^3x^2}\frac{\partial \xi}{\partial x} + 8\pi G\rho\xi + 2G\rho \int \frac{d^3x_3}{x_{31}} \frac{\partial^2}{\partial x_2{}^\alpha \partial x_3{}^\alpha} \zeta(1, 2, 3)\,. \tag{47}$$

An equation equivalent to this has been derived in another way (Peebles 1976*a*, eq. [23]; this equation differentiated with respect to x becomes eq. [47] above). We take equation (47) as the central equation for ξ in the numerical analysis. The two "difficult" terms are the last, which we write in terms of ξ by using equation (4), and the third, which involves the relative velocity dispersion. In the next section we derive a differential equation for this latter term.

e) A Dispersion Flux Equation

The result of multiplying equation (32) by $p_{21}{}^\beta p_{21}{}^\gamma$ and integrating over momenta is

$$\frac{\partial}{\partial t}\int p_{21}{}^\beta p_{21}{}^\gamma c(1,2)d^6p + \frac{1}{ma^2}\frac{\partial}{\partial x^\alpha}\int p_{21}{}^\alpha p_{21}{}^\beta p_{21}{}^\gamma c(1,2)d^6p + 4Gm^2n^2a^5A(x,t)x^\beta x^\gamma/x^3$$
$$+ 2Gm^2n^3a^8\int d^3x_3\,\frac{x_{31}{}^\beta x_{23}{}^\gamma}{x_{31}{}^3}A(x_{23}) + 4\frac{Gm^2}{a}\int\frac{d^3x_3}{x_{31}}\frac{\partial}{\partial x_3{}^\beta}\int d^9p\,p_{21}{}^\gamma d = 0\,. \quad (48)$$

The third and fourth terms have been simplified by using equation (42). As discussed in § VI, the first term measures the relative velocity dispersion in the directions perpendicular and parallel to the line joining the points 1 and 2. The second term measures the flux of the dispersion, and the remaining terms the effect of gravity.

f) Law of Conservation of Triplets

This is obtained by integrating equation (33) over all three momenta, using equation (22) to replace ρ_3 with the reduced correlation function d, and using equation (35) to eliminate the terms involving c. The result is

$$n^3a^9\frac{\partial\zeta}{\partial t} + \sum_{i=1,3}\frac{\partial}{\partial x_i{}^\alpha}\int d^9p\,\frac{p_i{}^\alpha}{ma^2}d = 0\,. \quad (49)$$

Just as equations (35) and (41) express conservation of particle pairs, equation (49) may be called a triplet conservation law.

g) Summary: The Limit $m \to 0$

As discussed in § II*e*, the equations are simplified by taking the limit $m \to 0$, $n \to \infty$ such that $\rho = nm =$ constant and ξ and ζ are fixed. By equations (10), (21), and (23), $p \propto m$, $c \propto n^2m^{-6}$, $d \propto n^3m^{-9}$, and $A \propto m$. Thus in this limit the second and third terms on the right side of equation (47) and the third term in equation (48) drop out. We summarize here the final set of equations on which the integration scheme is based (eqs. [42], [43], and [45] to [49]):

$$\left(\frac{d}{dt} + \frac{2}{a}\frac{da}{dt}\right)\frac{\langle p_1{}^2\rangle}{2m^2a^2} = \left(\frac{d}{dt} + \frac{1}{a}\frac{da}{dt}\right)\frac{G\rho a^2}{2}\int\frac{d^3x}{x}\xi\,; \quad (50a)$$

$$\int p_{21}{}^\alpha c d^6p = n^2a^6Ax^\alpha\,, \qquad \frac{\partial\xi}{\partial t} + \frac{1}{x^2a^2}\frac{\partial}{\partial x}\frac{(x^3A)}{m} = 0\,; \quad (50b)$$

$$\frac{\partial^2\xi}{\partial t^2} + \frac{2}{a}\frac{da}{dt}\frac{\partial\xi}{\partial t} + 8\pi G\rho\xi + \frac{\partial^2}{\partial x^\alpha\partial x^\beta}\int d^6p\,\frac{p_{21}{}^\alpha p_{21}{}^\beta}{m^2n^2a^{10}}c(1,2) + 2G\rho\int\frac{d^3x_3}{x_{31}}\frac{\partial^2}{\partial x_2{}^\alpha\partial x_3{}^\alpha}\zeta = 0\,; \quad (50c)$$

$$\frac{\partial}{\partial t}\int\frac{p_{21}{}^\beta p_{21}{}^\gamma c d^6p}{m^2n^2a^6} + \frac{\partial}{\partial x^\alpha}\int\frac{p_{21}{}^\alpha p_{21}{}^\beta p_{21}{}^\gamma}{m^3n^2a^8}c(1,2)d^6p$$
$$+ 2G\rho a^2\int d^3x_3\,\frac{x_{31}{}^\beta x_{23}{}^\gamma}{x_{31}{}^3}\frac{A(x_{23},t)}{m} + 4G\rho\int\frac{d^3x_3}{x_{31}}\frac{\partial}{\partial x_3{}^\beta}\int d^9p\,\frac{p_{21}{}^\gamma d}{mn^3a^7} = 0\,; \quad (50d)$$

$$\frac{\partial\zeta}{\partial t} + \sum_{i=1,3}\frac{\partial}{\partial x_i{}^\alpha}\int d^9p\,\frac{p_i{}^\alpha d}{mn^3a^{11}} = 0\,. \quad (50e)$$

By taking the limit $m \to 0$ in equation (47), for example, we are ignoring the direct gravitational interaction of particle pairs (third term on right side of eq. [47]) in favor of the acceleration due to all the other particles clustered about each particle pair (last two terms of eq. [47]). Equations (50) are not closed, but, as discussed in the following sections, they offer a reasonable guide to approximations that yield a tractable set of equations.

VI. TRUNCATION OF THE VELOCITY MOMENTS

The second momentum moment of $c(1, 2)$ occurs in equations (50c, d). This moment defines a second rank tensor which by symmetry has only two nonzero components. We define these components by functions $\Pi(x, t)$ and $\Sigma(x, t)$, given in Cartesian coordinates by

$$\frac{1}{n^2a^6}\int d^6p p_{21}{}^{\alpha}p_{21}{}^{\beta}c(x, p_1, p_2, t) \equiv \Sigma(x, t)\delta^{\alpha\beta} + [\Pi(x, t) - \Sigma(x, t)]\frac{x^{\alpha}x^{\beta}}{x^2}\cdot \tag{51}$$

Π and Σ are respectively the parallel and transverse (one dimension) correlated parts of the relative peculiar momentum dispersion of correlated particles. Π need not be equal to Σ, and indeed in the linear region of the solutions $\Pi \approx -n\Sigma$.

The physically observable function $\langle v_{21}{}^{\alpha}v_{21}{}^{\beta}\rangle$, the expectation value of the relative velocity dispersion of two particles as a function of their separation, is related to Π and Σ by consideration of the full two particle probability density (eq. [20])

$$\begin{aligned}\langle v_{21}{}^{\alpha}v_{21}{}^{\beta}\rangle &= \frac{\int d^6p[p_{21}{}^{\alpha}p_{21}{}^{\beta}/(ma)^2][\rho_1(1)\rho_1(2) + c(1, 2)]}{\int d^6p[\rho_1(1)\rho_1(2) + c(1, 2)]} \\ &= \frac{[\Sigma/(ma)^2 + 2/3\langle v_1{}^2\rangle]\delta^{\alpha\beta} + [(\Pi - \Sigma)/(ma)^2](x^{\alpha}x^{\beta}/x^2)}{1 + \xi(x, t)},\end{aligned} \tag{52}$$

where $\langle v_1{}^2\rangle$ (eq. [34]) is the proper peculiar velocity dispersion of particles.

Similarly, using equation (42) we can write $\langle \boldsymbol{v}_{21}\rangle$, the mean relative peculiar velocity of two particles separated by a comoving coordinate x, as

$$\langle \boldsymbol{v}_{21}\rangle = \frac{\int d^6p(\boldsymbol{p}_{21}/ma)[\rho_1(1)\rho_1(2) + c(1, 2)]}{\int d^6p[\rho_1(1)\rho_1(2) + c(1, 2)]} = \frac{\boldsymbol{x}A(x, t)/ma}{1 + \xi(x, t)}\cdot \tag{53}$$

Our velocity truncation procedure is to express the third moments, which occur in equation (50d), in terms of $\langle v_1{}^2\rangle$, A, Π, and Σ. This may be done if the skewness about the mean is 0. In one dimension we would have

$$\langle (v - \langle v\rangle)^3\rangle = 0 = \langle v^3\rangle - 3\langle v\rangle\langle v^2\rangle + 2\langle v\rangle^3\,. \tag{54}$$

In three dimensions, we note that $\langle \boldsymbol{v}_{21}\rangle = \boldsymbol{x}/x\langle v_{21}\rangle$, so that if we write

$$\langle (\boldsymbol{v}_{21} - \langle \boldsymbol{v}_{21}\rangle)^{\alpha}(\boldsymbol{v}_{21} - \langle \boldsymbol{v}_{21}\rangle)^{\beta}(\boldsymbol{v}_{21} - \langle \boldsymbol{v}_{21}\rangle)^{\gamma}\rangle = 0\,,$$

we have

$$\langle v_{21}{}^{\alpha}v_{21}{}^{\beta}v_{21}{}^{\gamma}\rangle = -2\langle v_{21}\rangle^3\frac{x^{\alpha}x^{\beta}x^{\gamma}}{x^3} + \langle v_{21}\rangle\left[\left(\frac{x^{\alpha}}{x}\langle v_{21}{}^{\beta}v_{21}{}^{\gamma}\rangle + \frac{x^{\beta}}{x}\langle v_{21}{}^{\alpha}v_{21}{}^{\gamma}\rangle + \frac{x^{\gamma}}{x}\langle v_{21}{}^{\alpha}v_{21}{}^{\beta}\rangle\right)\right]. \tag{55}$$

The desired moment of $c(1, 2)$ occurring in equation (50d) is related to $\langle v_{21}{}^{\alpha}v_{21}{}^{\beta}v_{21}{}^{\gamma}\rangle$ by

$$\langle v_{21}{}^{\alpha}v_{21}{}^{\beta}v_{21}{}^{\gamma}\rangle = \frac{\int d^6p[p_{21}{}^{\alpha}p_{21}{}^{\beta}p_{21}{}^{\gamma}/(ma)^3][\rho_1(1)\rho_1(2) + c(1, 2)]}{\int d^6p[\rho_1(1)\rho_1(2) + c(1, 2)]}\cdot \tag{56}$$

Using equations (52) and (53) in (55) and (56), we have

$$\begin{aligned}\int \frac{d^6p}{n^2a^6}p_{21}{}^{\alpha}p_{21}{}^{\beta}p_{21}{}^{\gamma}c(1, 2) = \frac{A}{1 + \xi}\Bigg\{&\left(3\Pi - 3\Sigma - \frac{2A^2x^2}{1 + \xi}\right)\frac{x^{\alpha}x^{\beta}x^{\gamma}}{x^2} \\ &+ [\Sigma + \tfrac{2}{3}\langle v_1{}^2\rangle(ma)^2](x^{\alpha}\delta\beta^{\gamma} + x^{\beta}\delta^{\alpha\gamma} + x^{\gamma}\delta^{\alpha\beta})\Bigg\}.\end{aligned} \tag{57}$$

VII. MODEL FOR THE THREE-POINT FUNCTION d

The three-point correlation function ζ which enters equation (50c) is the zeroth momentum moment of d, the reduced three-particle correlation function (eq. [23]). The first momentum moment of d occurs in equations (50d) and (50e), and to evaluate this we express d in terms of c in a manner consistent with equations (4), (23), (50b), and (50e). In this section we construct an analytic model for d consistent with these constraints.

First we express $c(1, 2)$ in terms of the average and relative momenta of the two particles,

$$\boldsymbol{p}_{21} = \boldsymbol{p}_2 - \boldsymbol{p}_1\,, \qquad \boldsymbol{P} = (\boldsymbol{p}_1 + \boldsymbol{p}_2)/2\,. \tag{58}$$

Assume that we can approximate $c(x, p_1, p_2, t)$ as a separable function of $\boldsymbol{p}_{21}$ and $\boldsymbol{P}$,

$$c(x, \boldsymbol{p}_1, \boldsymbol{p}_2, t) = C(x, \boldsymbol{p}_{21}, t)E(\boldsymbol{P}, t) . \tag{59}$$

This expression is not meant to be literally true; it is used only to arrive at a self-consistent model for the first moment of d (eq. [74]). By symmetry we have

$$\int E(\boldsymbol{P}, t)\boldsymbol{P} d^3P = 0 . \tag{60}$$

We shall normalize C and E according to

$$\int E(\boldsymbol{P}, t)d^3P = na^3 , \qquad \int C(x, \boldsymbol{p}_{21}, t)d^3p_{21} = \xi(x, t)na^3 . \tag{61}$$

No further information is needed about E; all the needed velocity moments are moments of $C(x, \boldsymbol{p}, t)$.

Equation (4) suggests we try writing d in terms of C as

$$d(1, 2, 3) = QE_3[(\boldsymbol{p}_1 + \boldsymbol{p}_2 + \boldsymbol{p}_3)/3, t][C(1, 2)C(2, 3) + C(2, 3)C(3, 1) + C(3, 1)C(1, 2)] . \tag{62}$$

The function E_3, like E, satisfies equations (60) and (61).

Equation (62) is obviously compatible with equation (4). To demonstrate its compatibility with equations (50b) and (50e), multiply equation (62) by the operator

$$\frac{1}{ma^2}\frac{\partial}{\partial x_1{}^\alpha}\int d^9p p_1{}^\alpha . \tag{63}$$

To evaluate the first term on the right side, transform to integration variables $\boldsymbol{p}_{12} \equiv \boldsymbol{p}_1 - \boldsymbol{p}_2$, $\boldsymbol{p}_{23} \equiv \boldsymbol{p}_2 - \boldsymbol{p}_3$, and $\boldsymbol{P} = (\boldsymbol{p}_1 + \boldsymbol{p}_2 + \boldsymbol{p}_3)/3$. The Jacobian of this transformation is $+1$. Then write

$$\boldsymbol{p}_1 = (2/3)\boldsymbol{p}_{12} + (1/3)\boldsymbol{p}_{23} + \boldsymbol{P} , \tag{64}$$

and we have for the first term on the right side of equation (62),

$$\begin{aligned} &\frac{Q}{ma^2}\frac{\partial}{\partial x_1{}^\alpha}\int d^3Pd^3p_{12}d^3p_{23}(2/3p_{12}{}^\alpha + 1/3p_{23}{}^\alpha + P^\alpha)C(1, 2)C(2, 3)E_3(P) \\ &\qquad = \frac{Qna^3}{ma^2}\frac{\partial}{\partial x_1{}^\alpha}\int d^3p_{12}d^3p_{23}(2/3p_{12}{}^\alpha + p_{23}{}^\alpha)C(1, 2)C(2, 3) \\ &\qquad = Qn^3a^9\left[-2/3\xi(2, 3)\frac{\partial}{\partial t}\xi(1, 2) + \frac{1}{3ma^2}x_{23}{}^\alpha A_{23}\frac{\partial}{\partial x_1{}^\alpha}\xi(1, 2)\right] , \end{aligned} \tag{65}$$

where for the last line we have used equations (37) and (42). Similarly, for the second term on the right side of equation (62) we write

$$\boldsymbol{p}_1 = -(2/3)\boldsymbol{p}_{31} - (1/3)\boldsymbol{p}_{23} + \boldsymbol{P} , \tag{66}$$

and we have

$$\begin{aligned} &\frac{Q}{ma^2}\frac{\partial}{\partial x_1{}^\alpha}\int d^3Pd^3p_{31}d^3p_{23}(-2/3p_{31}{}^\alpha - 1/3p_{23}{}^\alpha + P^\alpha)C(2, 3)C(3, 1)E_3(P) \\ &\qquad = Qn^3a^9\left[-2/3\xi(2, 3)\frac{\partial}{\partial t}\xi(3, 1) - \frac{1}{3ma^2}x_{23}{}^\alpha A_{23}\frac{\partial}{\partial x_1{}^\alpha}\xi(3, 1)\right] . \end{aligned} \tag{67}$$

For the third term of equation (62), write

$$\boldsymbol{p}_1 = \boldsymbol{P} - \boldsymbol{p}_{21}/3 - \boldsymbol{p}_{31}/3 , \tag{68}$$

which yields

$$\begin{aligned} &\frac{Q}{ma^2}\frac{\partial}{\partial x_1{}^\alpha}\int d^3Pd^3p_{12}d^3p_{31}(p_{12}{}^\alpha/3 - p_{31}{}^\alpha/3)C(3, 1)C(1, 2)E_3(P) \\ &\qquad = Qn^3a^9\left[-\tfrac{1}{3}\left(\xi_{31}\frac{\partial}{\partial t}\xi_{12} + \xi_{12}\frac{\partial}{\partial t}\xi_{13}\right) + \frac{1}{3ma^2}\left(A_{12}x_{12}{}^\alpha\frac{\partial}{\partial x_1{}^\alpha}\xi_{13} - A_{31}x_{31}{}^\alpha\frac{\partial}{\partial x_1{}^\alpha}\xi_{12}\right)\right] . \end{aligned} \tag{69}$$

Upon replacing $(\partial/\partial x_1{}^\alpha)p_1{}^\alpha$ by $(\partial/\partial x_2{}^\alpha)p_2{}^\alpha$ and $(\partial/\partial x_3{}^\alpha)p_3{}^\alpha$ in equation (63) and then adding the results, we have, after using equation (50e),

$$\frac{\partial}{\partial t}\zeta = Q\frac{\partial}{\partial t}(\xi_{12}\xi_{23} + \xi_{23}\xi_{31} + \xi_{31}\xi_{12}), \tag{70}$$

which is the desired result. All the last terms of equations (65), (67), and (69) have canceled in pairs. Therefore equation (62) is a self-consistent expression for d, properly expressing the conservation of triplets, and we can use it in equation (50d).

VIII. THE COMPLETE EQUATIONS

We can use the results of §§ VI and VII to write equations (50) in terms of five equations for the five unknowns $\xi(x, t)$, $\langle v_1{}^2(t)\rangle$, $A(x, t)$, $\Pi(x, t)$ and $\Sigma(x, t)$. We change to spherical coordinates where x is the distance between particles 1 and 2. Equations (50a)–(50c) become

$$\left(\frac{d}{dt} + \frac{2}{a}\frac{da}{dt}\right)\frac{\langle v_1{}^2\rangle}{2} = \left(\frac{d}{dt} + \frac{1}{a}\frac{da}{dt}\right)\frac{G\rho a^2}{2}\int\frac{d^3x}{x}\,\xi(x, t), \tag{71a}$$

$$\frac{\partial\xi}{dt} + \frac{1}{ma^2x^2}\frac{\partial}{\partial x}[x^3A(x, t)] = 0, \tag{71b}$$

$$\frac{\partial^2\xi}{\partial t^2} + \frac{2}{a}\frac{da}{dt}\frac{\partial\xi}{\partial t} - 8\pi G\rho\xi = \frac{1}{m^2a^4x^2}\frac{\partial}{\partial x}\left\{\frac{\partial}{\partial x}[x^2\Pi(x, t)] - 2x\Sigma(x, t)\right\} + 8\pi G\rho\mathscr{I}_1(x, t), \tag{72}$$

where we have defined

$$\begin{aligned}\mathscr{I}_1(x, t) &= \frac{1}{4\pi}\frac{\partial}{\partial x^\alpha}\int d^3z\frac{z^\alpha}{z^3}\zeta(x, z, |z - x|)\\ &= \frac{Q}{4\pi}\frac{\partial}{\partial x^\alpha}\int d^3z\frac{z^\alpha}{z^3}[\xi(x)\xi(z) + \xi(x)\xi(|x - z|) + \xi(z)\xi(|x - z|)]\\ &= \frac{Q}{4\pi}\frac{\partial}{\partial x^\alpha}\int d^3z\frac{z^\alpha}{z^3}\xi(|x - z|)[\xi(x) + \xi(z)].\end{aligned} \tag{73}$$

The last line of equation (73) follows by rotational symmetry.

The last term of equation (50d) is reduced using equation (62). We have

$$\begin{aligned}&\frac{4G\rho}{mn^3a^7}\int d^3x_{31}\frac{x_{31}{}^\alpha}{x_{31}{}^3}\int d^9pp_{21}{}^\beta d(1, 2, 3)\\ &= \frac{4G\rho a^2Q}{m}\int d^3z\frac{z^\alpha}{z^3}\{x^\beta A(x)[\xi(|x - z|) + \xi(z)] - (z - x)^\beta A(|z - x|)\xi(z) + z^\beta A(z)\xi(|x - z)|\}\\ &= \frac{8\pi G\rho a^2}{m}\left[\mathscr{I}_2(x)\frac{x^\alpha x^\beta}{x} + \mathscr{I}_3{}^{\alpha\beta}(x)\right],\end{aligned} \tag{74}$$

where we have defined the functions $\mathscr{I}_2$ and $\mathscr{I}_3{}^{\alpha\beta}$ as

$$\frac{x^\beta}{x}\mathscr{I}_2(x) \equiv \frac{Q}{2\pi}\int d^3z\frac{z^\beta}{z^3}[A(x)\xi(|z - x|) + A(|z - x|)\xi(z)], \tag{75a}$$

$$\mathscr{I}_3{}^{\alpha\beta}(x) = \frac{Q}{2\pi}\int d^3z\frac{z^\alpha z^\beta}{z^3}[A(z)\xi(|z - x|) - A(|z - x|)\xi(z)]. \tag{75b}$$

$\mathscr{I}_2$ is directed in the radial direction, whereas $\mathscr{I}_3{}^{\alpha\beta}$ has radial and isotropic components. $\mathscr{I}_3$ is much smaller than $\mathscr{I}_2$, and in the limit of a power law model for ξ, $A \propto \xi$ and $\mathscr{I}_3{}^{\alpha\beta}$ is zero.

If we take the divergence of equation (50d), we can eliminate the integral on the third term, and we have, using equation (51), (57), and (74),

$$
\begin{aligned}
\frac{\partial}{\partial t}\frac{1}{x^2}\left[\frac{\partial}{\partial x}(x^2\Pi) - 2x\Sigma\right] &+ \frac{3}{ax^2}\frac{\partial^2}{\partial x^2}[x^2 V(x,t)\Pi(x,t)] \\
&- \frac{6}{ax^3}\frac{\partial}{\partial x}[x^2 V(x,t)\Sigma(x,t)] + \frac{2m^2 a\langle v_1{}^2\rangle}{x^3}\frac{\partial}{\partial x}\left\{x^4\frac{\partial}{\partial x}\left[\frac{V(x,t)}{x}\right]\right\} \\
&- \frac{2m}{x^2}\frac{\partial^2}{\partial x^2}[x^3 V^2(x,t)A(x,t)] + 8\pi G\rho m a^2 x A(x,t) \\
&+ 8\pi G\rho Q m a^2\frac{1}{x^2}\frac{\partial}{\partial x}[x^3\mathscr{I}_2(x)] + 8\pi G\rho Q m a^2\frac{x^\alpha}{x}\frac{\partial}{\partial x^\beta}\mathscr{I}_3{}^{\alpha\beta}(x) = 0\,, \quad (76)
\end{aligned}
$$

where

$$V(x,t) = \frac{xA(x,t)/ma}{1+\xi(x,t)}\,, \quad (77)$$

and where the repeated indices α and β in the last term are summed over.

A final independent equation can be derived from the transverse component of equation (50d), that is, the part perpendicular to $x^\alpha x^\beta$.

Defining a perpendicular projection operator $\Delta^{\alpha\beta}$ by

$$\Delta^{\alpha\beta} = \frac{1}{2}\left(\delta^{\alpha\beta} - \frac{x^\alpha x^\beta}{x^2}\right), \quad (78)$$

we can multiply equation (50d) by $\Delta^{\alpha\beta}$, which gives

$$
\begin{aligned}
\frac{\partial}{\partial t}\Sigma(x,t) &+ \frac{1}{ax^4}\frac{\partial}{\partial x}\{x^4 V(x,t)\,[\Sigma(x,t) + \tfrac{2}{3}(ma)^2\langle v_1{}^2\rangle]\} \\
&- \frac{8\pi}{3}G\rho m a^2\left[\frac{1}{x^3}\int_0^x dz z^4 A(z) + \int_x^\infty dz z A(z)\right] + 8\pi G\rho m a^2\mathscr{I}_3{}^{\alpha\beta}\Delta^{\alpha\beta} = 0\,, \quad (79)
\end{aligned}
$$

where repeated indices are summed. The angular integral on the third term of equation (50d) has been analytically reduced to yield the third term of equation (79).

Equations (71), (72), (76), and (79) define a system of five equations and five unknowns. The system is a nonlinear, integrodifferential initial value problem that can be solved for a given set of initial conditions at some specified starting time. As discussed in § II*d*, we fix initial conditions through the similarity solution derived in the next section.

IX. THE SIMILARITY TRANSFORMATION

The similarity solution is based on the time scaling in the Einstein–de Sitter universe,

$$H = (da/dt)/a = 2/3t\,, \qquad 8\pi G\rho = 4/3t^2\,. \quad (80)$$

The scaling relations are

$$
\begin{aligned}
\rho_1(p,t) = t^{-3\beta}l(p/t^\beta)\,, \qquad c(\boldsymbol{x},\boldsymbol{p}_1,\boldsymbol{p}_2,t) = t^{-6\beta}g(x/t^\alpha,\boldsymbol{p}_1/t^\beta,\boldsymbol{p}_2/t^\beta)\,, \\
d(\boldsymbol{x}_1,\boldsymbol{x}_2,\boldsymbol{x}_3,\boldsymbol{p}_1,\boldsymbol{p}_2,\boldsymbol{p}_3) = t^{-9\beta}h(\boldsymbol{x}_1/t^\alpha,\boldsymbol{x}_2/t^\alpha,\boldsymbol{x}_3/t^\alpha,\boldsymbol{p}_1/t^\beta,\boldsymbol{p}_2/t^\beta,\boldsymbol{p}_3/t^\beta)\,, \quad (81)
\end{aligned}
$$

where α and β are constants related by

$$\beta = \alpha + 1/3\,. \quad (82)$$

Equations (81) yield the scaling relations for the spatial functions (eqs. [18], [21], [23]),

$$\int l(p')d^3p' = na^3 = \text{constant}\,, \qquad \xi(x,t) = \boldsymbol{\xi}(x/t^\alpha)\,, \qquad \zeta(x_{12},x_{23},x_{31},t) = \boldsymbol{\zeta}(x_{12}/t^\alpha, x_{23}/t^\alpha, x_{31}/t^\alpha)\,. \quad (83)$$

As indicated, in the similarity solution $\boldsymbol{\xi}$ and $\boldsymbol{\zeta}$ are functions of the scaled variable x/t^α only. The result of substituting equations (80)–(83) into equations (50) is to produce a set of equations in the independent variables $s = x/t^\alpha$, $\boldsymbol{p}' = \boldsymbol{p}/t^\beta$, the time no longer appearing explicitly. In a solution to these scaled equations, characteristic coordinate lengths scale with time as t^α, proper lengths as $at^\alpha \propto t^{(\alpha+2/3)}$, proper velocities as $t^\beta/a \propto t^{(\alpha+2/3)}/t$; canonical momenta scale as t^β, consistent with $\beta = \alpha + 1/3$.

Equations (80)–(82) are solutions to equation (50) for any value of the parameter α. We constrain α by the asymptotic boundary conditions.

At large separation x the correlation function is given by the linear perturbation result (eq. [6]). This, combined with the second of equations (83), says

$$\xi \propto t^{4/3}x^{-(3+n)} = \boldsymbol{\xi}(x/t^{\alpha}), \qquad \xi \ll 1,$$

so

$$\alpha = 4/(9 + 3n). \tag{84}$$

We assume that at small x, where $\xi \gg 1$, the particle pairs generally are in the same gravitationally bound and stable cluster. This would say that the mean rate of proper separation of the pairs is close to zero, or, since v (eq. [40]) is measured relative to the general expansion, that

$$v = -\frac{2}{3t}a(t)x, \qquad \xi \gg 1. \tag{85}$$

This expression in the pair conservation law (eq. [41]) with $\xi = \boldsymbol{\xi}(x/t^{\alpha}) \gg 1$ gives

$$\frac{d\boldsymbol{\xi}}{ds} = -\frac{2}{\alpha + 2/3}\frac{\boldsymbol{\xi}}{s}, \qquad s = x/t^{\alpha},$$

whence

$$\boldsymbol{\xi} \propto s^{-\gamma}, \qquad \gamma = 2/(\alpha + 2/3). \tag{86}$$

By equations (84) and (86),

$$\gamma = (9 + 3n)/(5 + n), \tag{87}$$

as in equation (7).

In summary, the similarity solutions to equation (50) are parametrized by the spectral index n of small perturbations, in conjunction with the following boundary conditions: (1) stability of the bound clusters at small separations, and (2) asymptotic agreement with linear perturbation theory at large separation. In the similarity solutions, $\boldsymbol{\xi}(s) \propto s^{-\gamma}$ for $\boldsymbol{\xi} \gg 1$, and $\boldsymbol{\xi}(s) \propto s^{-(3+n)}$ for $\boldsymbol{\xi} \ll 1$.

The stability boundary condition at small separation is the only physically reasonable condition one could impose. Our truncation scheme for the velocity moments has deleted those terms which describe the subsequent relaxation of virialized systems, so the imposed boundary condition is the only condition physically consistent with our equations.

In the similarity solution it is convenient to introduce new scaled functions and a new independent variable,

$$\begin{gathered} s = ax/t^{\alpha+2/3} \propto xt^{-\alpha}, \qquad \xi(x, t) = \boldsymbol{\xi}(s), \qquad A(x, t) = ma^2t^{-1}\boldsymbol{A}(s), \\ \Pi(x, t) = m^2a^2t^{2\alpha-2/3}\boldsymbol{\Pi}(s) = (ma)^2(ax/st)^2\boldsymbol{\Pi}(s), \\ \Sigma(x, t) = m^2a^2t^{2\alpha-2/3}\boldsymbol{\Sigma}(s), \qquad \langle v_1{}^2(t)\rangle = a^2t^{2\alpha-2}\boldsymbol{K} = (ax/st)^2\boldsymbol{K}. \end{gathered} \tag{88}$$

As may be verified by using equations (81)–(83) in equations (10), (17), (42), and (51), $\boldsymbol{\xi}$, $\boldsymbol{A}$, $\boldsymbol{\Sigma}$, and $\boldsymbol{\Pi}$ are functions of s alone and $\boldsymbol{K}$ is a constant. These new functions are independent of m and they are independent of the units of the "unphysical" coordinate x; that is, they are unchanged if a is multiplied by a fixed factor but ax held fixed. On using equations (80) and (88) in equations (71), (72), (76), and (79), we find

$$\boldsymbol{K} = \frac{2\alpha}{3\alpha + 1}\int_0^{\infty} s'\boldsymbol{\xi}(s')\,ds', \tag{89a}$$

$$-\alpha s\frac{d}{ds}\boldsymbol{\xi}(s) + \frac{1}{s^2}\frac{d}{ds}[s^3\boldsymbol{A}(s)] = 0, \tag{89b}$$

$$\alpha^2 s\frac{d}{ds}\left[s\frac{d}{ds}\boldsymbol{\xi}(s)\right] - \frac{\alpha}{3}s\frac{d}{ds}\boldsymbol{\xi} - (4/3)\boldsymbol{\xi} = \frac{1}{s^2}\frac{d}{ds}\left\{\frac{d}{ds}[s^2\boldsymbol{\Pi}(s)] - 2s\boldsymbol{\Sigma}(s)\right\} + (4/3)\mathscr{I}_1(s), \tag{89c}$$

$$\begin{aligned} &\left(\alpha + \tfrac{2}{3} - \alpha s\frac{d}{ds}\right)\left\{\frac{1}{s^2}\frac{d}{ds}[s^2\boldsymbol{\Pi}(s)]\right\} + \frac{3}{s^2}\frac{d^2}{ds^2}[s^2V(s)\boldsymbol{\Pi}(s)] - \frac{2}{s}\left(2\alpha + \tfrac{2}{3} - \alpha s\frac{d}{ds}\right)\boldsymbol{\Sigma}(s) - \frac{6}{s^3}\frac{d}{ds}[s^2V(s)\boldsymbol{\Sigma}(s)] \\ &\quad + \frac{2\boldsymbol{K}}{s^3}\frac{d}{ds}s^4\frac{d}{ds}\frac{V(s)}{s} - \frac{2}{s^2}\frac{d^2}{ds^2}[s^3V^2(s)\boldsymbol{A}(s)] + (4/3)s\boldsymbol{A}(s) + 4/3\mathscr{I}_4(s) + 4/3\left(\frac{s^{\nu}}{s}\right)\frac{d}{ds^{\mu}}\mathscr{I}_3{}^{\mu\nu}(s) = 0, \end{aligned} \tag{89d}$$

$$\begin{aligned} &\left(2\alpha + \tfrac{2}{3} - \alpha s\frac{d}{ds}\right)\boldsymbol{\Sigma}(s) + \frac{1}{s^4}\frac{d}{ds}\{V(s)s^4[\boldsymbol{\Sigma}(s) + 2/3\boldsymbol{K}]\} \\ &\quad - 4/9\left[\frac{1}{s^3}\int_0^s ds'(s')^4\boldsymbol{A}(s') + \int_s^{\infty} ds's'\boldsymbol{A}(s)\right] + \tfrac{4}{3}\mathscr{I}_3{}^{\mu\nu}(s)\Delta^{\mu\nu} = 0, \end{aligned} \tag{89e}$$

where we have defined

$$V(s) = \frac{sA(s)}{1 + \xi(s)}, \tag{90a}$$

$$\mathscr{I}_4(s) = \frac{1}{s^2}\frac{d}{ds}s^2\mathscr{I}_2(s). \tag{90b}$$

$\mathscr{I}_1$, $\mathscr{I}_2$, and $\mathscr{I}_3$ have the forms given in equations (73) and (75) save that A is replaced with A and $\boldsymbol{x}$ with s.

X. SIMPLIFICATION OF THE INTEGRAL TERMS

Equations (89a)–(89e) are still extremely difficult to solve because $\mathscr{I}_1$, $\mathscr{I}_2$, and $\mathscr{I}_3$ are integral operators that are nontrivial in two dimensions. If, however, $\zeta(1, 2, 3)$ (or, equivalently, ξ via eq. [4]) assumes a power law shape, then $\mathscr{I}_1(s)$ and $\mathscr{I}_4(s)$ can be reduced to differential operators, and $\mathscr{I}_3{}^{\alpha\beta} = 0$. This then enables one to solve the equations using standard one-dimensional boundary value techniques. Except for equations (89a) and (89e), the equations become local, which greatly simplifies the numerical analysis.

$\mathscr{I}_1$ and $\mathscr{I}_4$ are on the order of ξ^2 and so are dominant when $\xi \gg 1$, and negligible when $\xi \ll 1$. The expected solution for ξ is a power law when $\xi \gg 1$. If we replace $\mathscr{I}_1$ and $\mathscr{I}_4$ by differential operators valid when ξ is a power law, then our expressions for these terms will be correct when $\xi \gg 1$, but will not be correct when ξ departs from a power law at $\xi \approx 1$. In this transition zone, however, the integral terms $\mathscr{I}_1$ and $\mathscr{I}_4$ are becoming unimportant in equations (89), and furthermore, in this region we can no longer justify equation (4), the expression of ζ in terms of ξ.

Therefore, in order to facilitate the numerical solution of equation (89), it is not unreasonable in this first discussion of the equations to replace one approximation that is difficult to compute by another approximation which is easier to compute. Both the integral operators, and the differential operators that replace them, are accurate when $\xi \gg 1$. Neither is expected to be exactly correct when $\xi \lesssim 1$.

The expressions for $\mathscr{I}_1(s)$ and $\mathscr{I}_2(s)$ given by equations (73) and (75) can be readily evaluated when ξ has a power law form. If $\xi(s) = B/s^\gamma$, we have

$$\mathscr{I}_1(s) = \frac{QB^2}{4\pi}\frac{\partial}{\partial s^\alpha}\int d^3z\,\frac{z^\alpha}{z^3}\frac{1}{(|s - z|)^\gamma}\left(\frac{1}{z^\gamma} + \frac{1}{s^\gamma}\right) = \frac{Q}{s^2}\frac{d}{ds}\,[s^3\xi(s)^2 M_\gamma]\,, \tag{91}$$

where

$$M_\gamma = [2(2 - \gamma)(4 - \gamma)]^{-1}\int \frac{dy}{y^2}\left(1 + \frac{1}{y^\gamma}\right) \times \{(1 + y)^{4-\gamma} - |1 - y|^{4-\gamma} - (4 - \gamma)y[(1 + y)^{2-\gamma} - |1 - y|^{2-\gamma}]\}\,. \tag{92}$$

With $\xi(s)$ a power law, equation (91) is equivalent to

$$\mathscr{I}_1(s) = Q(3 - 2\gamma)M_\gamma\xi^2(s)\,. \tag{93}$$

Since $\xi(s)$ is expected to depart from a power law when $\xi \approx 1$, equations (91) and (93) will not be equivalent in this region, and M_γ will itself be a function of s. However, we emphasize again that the observational justification for equation (4) is rather weak when $\xi \approx 1$, so we are not introducing much additional uncertainty by simplifying $\mathscr{I}_1(s)$ to equation (91) or (93).

A similar reduction can be applied to $\mathscr{I}_4(s)$ by noting that in the power law model $A(s)/\xi(s) =$ constant. The result is

$$\mathscr{I}_4(s) = QM_\gamma\frac{1}{s^2}\frac{d}{ds}\,[s^4A(s)\xi(s)]\,, \tag{94}$$

or, equivalently, in the power law model,

$$\mathscr{I}_4(s) = (4 - 2\gamma)QM_\gamma sA(s)\xi(s)\,. \tag{95}$$

In the power law model all components of $\mathscr{I}_3{}^{\alpha\beta}(s)$ vanish.

Since $\gamma < 2$ when $\xi \gg 1$, and $\gamma > 2$ when $\xi \ll 1$, $\mathscr{I}_4(s)$ as given by equation (94) changes sign beween the linear and nonlinear solutions, whereas no sign change occurs in equation (95). These two expressions for $\mathscr{I}_4$ are thus very different when $\xi \lesssim 1$, and an important check on our model is to see whether the solutions are also strongly dependent on the form of $\mathscr{I}_4$. Another check is to compare solutions obtained using equations (91) and (93) for $\mathscr{I}_1$, although here no sign change occurs in either expression if the logarithmic derivative of ξ is less than -1.5. As described below (§ XIII), the different reductions of $\mathscr{I}_4$ do not seriously affect the solutions. However, because of the shape of ξ in the transition region, equations (91) and (93) for $\mathscr{I}_1$ behave very differently, and in fact no solutions satisfying the boundary conditions were found using equation (91).

XI. ASYMPTOTIC SOLUTIONS

a) $\xi \ll 1$

In the limit of $\xi \ll 1$, equations (89) must reduce to linear perturbation theory. All the nonlinear terms of equations (89) vary as ξ^2, and can be neglected. The equations become

$$-\alpha s \frac{d}{ds}\xi + \frac{1}{s^2}\frac{d}{ds}(s^3 A) = 0\,, \tag{96a}$$

$$\alpha^2 s \frac{d}{ds}\left(s\frac{d}{ds}\xi\right) - \frac{\alpha}{3}s\frac{d}{ds}\xi - 4/3\xi = \frac{1}{s^2}\frac{d}{ds}\left\{\frac{d}{ds}[s^2\mathbf{\Pi} - 2s\mathbf{\Sigma}(s)]\right\}, \tag{96b}$$

$$\left(3\alpha + \tfrac{2}{3} - \alpha s\frac{d}{ds}\right)\left[\frac{d}{ds}(s^2\mathbf{\Pi}) - 2s\mathbf{\Sigma}\right] + \tfrac{4}{3}s^3 A(s) = 0\,, \tag{96c}$$

$$\left(2\alpha + \tfrac{2}{3} - \alpha s\frac{d}{ds}\right)\mathbf{\Sigma}(s) - \frac{4}{9}\left[\frac{1}{s^3}\int_0^s ds'(s')^4 A(s') + \int_s^\infty ds' s' A(s')\right] = 0\,. \tag{96d}$$

Equations (96a)–(96c) are three equations in the three unknowns ξ, A, and $\mathscr{L} \equiv (d/ds)(s^2\mathbf{\Pi}) - 2s\mathbf{\Sigma}$. Since the equations are equidimensional, the most general solutions will be power laws, $\xi \propto A \propto s^{-\delta}$, $\mathscr{L} \propto s^{3-\delta}$, $\mathbf{\Pi} \propto \mathbf{\Sigma} \propto s^{2-\delta}$. Equations (96a)–(96c) define an eigenvalue problem for δ, with solutions given by setting the determinant of the defining matrix to 0. This factors to

$$(\alpha\delta - \tfrac{4}{3})(\alpha\delta + \tfrac{1}{3})(\alpha\delta + 2)(\delta - 3) = 0\,. \tag{97}$$

The first solution is the desired one, since it implies $\xi(x, t) \propto t^{4/3}$, in accordance with the growing mode of linear perturbation theory. Linear perturbation theory also predicts density fluctuations that decay as t^{-1}, and since $\xi \propto |\delta\rho/\rho|^2$, there exist solutions where ξ varies as t^{-2} and as $t^{-1/3}$ for the purely decaying and the mixed modes, respectively. These modes correspond to the second and third parentheses of equation (97). The $\delta = 3$ solution does not correspond to density fluctuations, since it gives $\xi = 0$. There also exists a $\delta = 4$ mode which is purely a homogeneous $\mathbf{\Pi}$ solution, with $A = \xi = 0$.

In the two solutions involving decaying modes, ξ increases with increasing spatial separation (increasing s). As discussed in § II, we adopt the pure growing mode, that is, we take $\alpha\delta = 4/3$, so $\xi \propto s^{-\delta}$, $\delta = 3 + n$ (eq. [84]), and by equation (96),

$$A = 4\xi/(3n)\,, \qquad \mathbf{\Sigma} = \frac{8s^2\xi}{9n(2-n)(1+n)}\,, \qquad \mathbf{\Pi} = -n\mathbf{\Sigma}\,. \tag{98}$$

These are the boundary conditions at large s.

Since we will be assuming $n \approx 0$, there is in the linear region a significant anisotropy of the correlated components of the relative velocity dispersion of pairs. For $-1 < n < 0$, both $\mathbf{\Pi}$ and $\mathbf{\Sigma}$ are negative, indicating that the relative velocity dispersion for particles separated by distance s is slightly less than the relative dispersion of random particle pairs at very large separation (see eq. [52]). This is true both in the transverse and radial directions. For $0 < n < 2$, $\xi(s)$ is negative at large s, and $\mathbf{\Sigma}(s)$ is also negative, but now $\mathbf{\Pi}(s)$ is positive. This in turn implies that the radial relative velocity dispersion is above the random value, and the transverse relative dispersion is below the random value.

b) $\xi \gg 1$

In the limit $\xi \gg 1$, equations (89) again simplify considerably. Keeping the highest order terms in each equation, we have

$$-\alpha s \frac{d}{ds}\xi + \frac{1}{s^2}\frac{d}{ds}(s^3 A) = 0\,, \tag{99a}$$

$$\frac{1}{s^2}\frac{d}{ds}\left[\frac{d}{ds}(s^2\mathbf{\Pi}) - 2s\mathbf{\Sigma}\right] = (4/3)(2\gamma - 3)QM_\gamma\xi^2\,, \tag{99b}$$

$$\left(\alpha + \tfrac{2}{3} - \alpha s\frac{d}{ds}\right)\frac{1}{s^2}\frac{d}{ds}(s^2\mathbf{\Pi}) + \frac{3}{s^2}\frac{d^2}{ds^2}(s^2 V\mathbf{\Pi}) - (2/s)\left[2\alpha + \tfrac{2}{3} - \alpha s\frac{d}{ds}\right]\mathbf{\Sigma} - \frac{6}{s^3}\frac{d}{ds}(s^2 V\mathbf{\Sigma}) + \tfrac{8}{3}(4 - 2\gamma)QM_\gamma s A\xi = 0\,, \tag{99c}$$

$$\left(2\alpha + \tfrac{2}{3} - \alpha s\frac{d}{ds}\right)\mathbf{\Sigma} + \frac{1}{s^4}\frac{d}{ds}[s^4 V(s)\mathbf{\Sigma}] = 0 \tag{99d}$$

$$V = sA/\xi\,. \tag{99e}$$

Here we have reduced $\mathscr{I}_1$ and $\mathscr{I}_4$ according to equations (93) and (95). The mean relative peculiar velocity of particles separated by distance x is $axA/(t\xi)$ when $\xi \gg 1$ (eqs. [40], [42], and [88]). By hypothesis and our truncation scheme discussed above, this velocity should just cancel the Hubble flow $\frac{2}{3}(ax/t)$ because the particles are expected to be in stable clusters. Therefore $A(s)/\xi(s) = -2/3$ and $V = -2s/3$. By equation (99a), this can occur only if $\xi(s)$ varies as a power of s, and, as discussed in § IX, equation (99a) fixes the power law index in terms of α, and hence n (eqs. [86] and [87]).

Equation (99d) is a first-order homogeneous equation for $\mathbf{\Sigma}(s)$. Since it is equidimensional in s the solution is a power law which, when $V = -2s/3$, reduces to $\mathbf{\Sigma} \propto s^{2-2\gamma}$. Equations (99b) and (99c) are also equidimensional, and also imply that $\mathbf{\Pi}(s)$ will have a power law solution $\mathbf{\Pi} \propto s^{2-2\gamma}$. For this power law solution, both equations (99b) and (99c) reduce to an algebraic relation between ξ, $\mathbf{\Pi}$, and $\mathbf{\Sigma}$,

$$\mathbf{\Sigma}(s) - (2 - \gamma)\mathbf{\Pi}(s) = (2/3QM_\gamma)s^2\xi^2(s)\,. \tag{100}$$

$\mathbf{\Sigma}$ and $\mathbf{\Pi}$ should of course be positive in this domain and M_γ is positive over the domain of γ we shall consider. In this asymptotic limit the physical velocity dispersions $\langle v_{21}{}^2\rangle$ (see eqs. [52]) in the parallel and perpendicular directions will be given by

$$\langle v_{21}{}^\alpha v_{21}{}^\beta\rangle \approx \delta^{\alpha\beta}\mathbf{\Sigma}(s)/\xi(s) + \frac{x^\alpha x^\beta}{x^2}[\mathbf{\Pi}(s) - \mathbf{\Sigma}(s)]/\xi(s)\,, \tag{101}$$

and by equation (100) the ratio of velocity dispersions in the radial and transverse directions is

$$\langle v_t{}^2\rangle/\langle v_r{}^2\rangle = 2 - \gamma + 2QM_\gamma s^2\xi^2/3\mathbf{\Pi}\,. \tag{102}$$

The solution in this limiting case does not constrain the velocity dispersions to be isotropic, that is, $\langle v_r{}^2\rangle = \langle v_t{}^2\rangle$; rather, the value of the constant $s^2\xi^2/\mathbf{\Pi}$ depends on the join to the solutions valid in the limit $s \to \infty$. This agrees with van Albada's (1960, 1961) argument that in large clusters the velocity dispersion could be expected to be larger in the transverse than in the radial directions relative to the cluster center because of centrifugal force and the conservation of angular momentum.

c) *Eigenvalues*

In the linear asymptotic region, the amplitude of ξ at a coordinate point completely specifies the solution (eqs. [98]). The nonlinear asymptotic solution is completely determined via two parameters, for example the values of ξ and $\mathbf{\Sigma}$ at a specified point. We seek a solution that smoothly joins the two asymptotic solutions, and for this we must solve equations (89) numerically.

Consider for a moment equations (89) as an initial value problem for which we prescribe initial values at some small s, according to the desired asymptotic behavior in this limit. If the equation is integrated toward large s eventually the nonlinear terms will lose importance, and the solution will become a linear superposition of power laws with indices δ fixed by equation (97). In general this solution will contain negative values of δ, so the solution will blow up at infinite spatial separation ($s \to \infty$). Conversely, if we start at large s, with the wanted linear solution and integrate inward, there is no guarantee that the solution will settle down to a power law at $\xi \gg 1$. If it does not, then v cannot be arranged to cancel the Hubble flow, so the wanted stability condition cannot be satisfied. The boundary value problem thus is an eigenvalue problem. Only for selected values of parameters defining the equations can solutions exist which have the desired asymptotic boundary conditions. Of course it is always possible that there are no eigenvalues which produce the desired solution. With this highly nonlinear system, the proof of an existence theorem would be extremely difficult.

In our system of equations as formulated, there is only one parameter which is not completely specified and which can serve as an eigenvalue. This parameter is Q, which measures the strength of the three-point correlations in terms of the two-point correlations. One reason for thinking Q might be the key parameter is the fact that the velocity dispersion depends on Q when $\xi \gg 1$ (eq. [100]) but is independent of Q when $\xi \ll 1$. Thus there exists a value of Q for which the match of dispersions at the transition region $\xi \approx 1$ is best. This still does not guarantee the existence of a solution having the desired boundary conditions at both asymptotes, but we do find that, within the accuracy of the numerical integration, the desired solutions usually do exist.

Thus an extremely important outcome of this calculation is the eigenvalue of Q which yields solutions having the proper asymptotic solutions. Q is an observable parameter, and it will serve as a check on the theory to see if the eigenvalues of Q are within the observed limits. It is also clear that the eigenvalue of Q may depend on which reduction scheme for $\mathscr{I}_1$ and $\mathscr{I}_4$ is used because the different reductions behave differently when $\xi \approx 1$.

XII. NUMERICAL TECHNIQUE

To solve equations (89) we first transform to a logarithmic coordinate u,

$$u = \ln s\,, \qquad \frac{d}{du} = s\frac{d}{ds}\,, \tag{103}$$

and convert the equations to difference equations. Second-order differences are employed for equations (89b, c, d) but in equation (89e), where it is necessary only to specify a boundary condition at large s, we use first-order forward differences. The difference grid consists of 200 points, with the step increment $du = 0.05$, so s varies from 0.01 to ~ 209.

Boundary conditions are chosen so $\xi \approx 1$ occurs near the midrange of the grid. This insures that the equations are well described by their asymptotic limits at each boundary. At the small s boundary we specify ξ, $\boldsymbol{A}$, $d\xi/du$, and $(d/du)(\ln \boldsymbol{\Pi})$. At the large s boundary we specify the logarithmic derivative $(d/du)(\ln \xi)$. The remaining parameters at large s are specified as three algebraic equations between $\boldsymbol{A}$, $\boldsymbol{\Pi}$, $\boldsymbol{\Sigma}$, and ξ at the boundary. These are the expressions appropriate to the desired solution $\alpha\delta = 4/3$ in the large s limit. We are solving three second-order equations and one first-order equation, so we have seven free parameters to specify plus one additional parameter to scale the overall solutions, since there are no inhomogeneous source terms in equations (89). Four of these degrees of freedom are taken up at the small s boundary, and the remaining four are specified at the large s boundary.

The expected solutions for ξ, $\boldsymbol{A}$, $\boldsymbol{\Pi}$, and $\boldsymbol{\Sigma}$ vary by large factors between the small s and large s limits. To improve the accuracy of the numerical solutions we solve the equations in terms of the functions $s^2\xi(s)$, $s^2\boldsymbol{A}(s)$, $s\boldsymbol{\Pi}(s)$, and $s\boldsymbol{\Sigma}(s)$. The variation of these functions over the range of s is considerably less than the original functions.

The various integral terms appearing in equation (89) imply that the matrix describing the difference equations is not sparse, and in general the equations must be solved by matrix inversion techniques. The number of computational steps required to solve n simultaneous equations on m grid points is proportional to $(nm)^2$, if the defining matrix is nonsparse. In the absence of the integral terms, the defining matrix is block tridiagonal, and can be readily solved by factoring the matrix into a product of two bidiagonal matrices (see, e.g., Acton 1970). The total number of computations and steps required for solution of a block tridiagonal system is proportional to n^2m, a factor of some 200 reduction in computing time in our situation.

Equation (91e) contains an integral term, which we convert into a local term by defining a new function $\boldsymbol{J}(s)$,

$$s^2\boldsymbol{A}(s)\boldsymbol{J}(s)\left(\frac{1}{2-n}+\frac{1}{1+n}\right) \equiv \frac{1}{s^3}\int_0^s dz z^4 \boldsymbol{A}(z) + \int_s^\infty dz z \boldsymbol{A}(z)\,. \tag{104}$$

In the asymptotic solution at large s, $\boldsymbol{A}(s) \propto s^{-(3+n)}$ and $\boldsymbol{J}(s) = 1$. In the nonlinear region $\boldsymbol{J}(s)$ is greater than 1. The term is important, however, only in the linear region, and so a good approximation is to set $J(s) = 1$. We also convert $\mathscr{I}_1(s)$ and $\mathscr{I}_4(s)$ into local operators as described above, and we set $\mathscr{I}_3{}^{\mu\nu}(s) = 0$. The full function $\boldsymbol{J}(s)$ can be readily found, given $A(s)$, so it is possible to iterate the solutions until equation (104) is explicitly solved. Some solutions were generated where $\boldsymbol{J}(s)$ was iterated via equation (104), and will be discussed below.

The nonlinear terms in equations (89) are handled by Newton-Raphson linearization. Terms containing $\boldsymbol{K}$ are significant in the transition zone, and equation (89a), which defines $\boldsymbol{K}$, is intrinsically nonlocal. The iteration of $\boldsymbol{K}$ necessarily lags behind the other functions. Given the ith iteration of ξ—call it ξ^i—we compute $\boldsymbol{K}^i$ via equation (89a), and use $(\boldsymbol{K}^i + \boldsymbol{K}^{i-1})/2$ as the estimator of $\boldsymbol{K}$ for the next iteration of ξ and the other functions. Because $\boldsymbol{K}$ lags, our convergence rate for the iterations is far below the usual convergence of Newton-Raphson linearization. Nevertheless, the computing time required to reach convergence to 1% accuracy is relatively short. If we ignore the fifth and sixth terms of equation (89d), which are negligible except when $\xi \approx 1$, we reach convergence to 1% accuracy in usually less than 30 iterations, starting with a reasonable guess for the zeroth level iteration. Including these two terms greatly increases the number of iterations required for convergence. We find, however, that the solution including these two terms does not vary significantly from the solution ignoring these terms, and in order to reduce computing costs, most of the solutions discussed below were computed ignoring these two terms.

In the first step of the computation we obtain trial solutions based on $Q = 1$. The result always satisfies the boundary conditions but usually the solution exhibits a discontinuity at the small s boundary, and the logarithmic derivative of ξ at $\xi \gg 1$ does not reach a constant value or else reaches a value different from the wanted γ—that is, the stability condition is not satisfied. Generally, however, by slowly varying Q we generate a series of solutions, and we can find a value for which ξ, $\boldsymbol{\Pi}$, and $\boldsymbol{\Sigma}$ have the wanted asymptotic behavior.

XIII. NUMERICAL RESULTS

a) Choice of the Power Spectrum Index n

We have solved the equation for various values of the free parameter n, the spectral index of the initial density perturbation (eq. [5]). Convergence of the rms single particle velocity dispersion (eq. [89a]) requires $-1 \leq n \leq 1$. The observational data suggest $n \approx 0$ (Peebles 1974). Since the particular numerical method adopted here fails if $n = 0$ (because ξ goes to zero at $s \to \infty$ faster than a power law when $n = 0$), the results presented here are based on $n = -0.1$ ($\gamma = 1.776$). We find that results for $n = 0.1$ and $n = -0.1$ are very similar over the range of interesting values of s, and, since there is no physical discontinuity at $n = 0$, we expect that the results presented here are an adequate approximation to the case $n = 0$.

TABLE 1

PARAMETERS AND RESULTS OF MODEL SOLUTIONS

Model No. (1)	$\mathscr{I}_1$ (2)	$\mathscr{I}_4$ (3)	All Terms (4)	ξ_{MAX} (5)	ξ_{BEND} (6)	Q (7)	$\langle v_r^2\rangle/\langle v_t^2\rangle$ (8)
1............	Aa	Aa	No	0.66	0.10	0.72	0.89
2............	Aa	Da	No	0.47	0.25	0.58	1.15
3............	Aa	Da	Yes	0.42	0.25	0.62	1.0
4............	Ab	Da	No	0.064	...	1.28	0.69
5............	Ab	Db	No	0.038	...	0.97	1.20
6............	Ac	Da	No	0.70	0.25	0.40	1.58
7............	Ac	Dc	No	1.18	0.14	0.48	1.12

b) Comparisons of Results for Different Methods of Approximation

An essential first test is to determine the sensitivity of the central results, the value of Q and the shape of ξ, to the methods of approximating $\mathscr{I}_1$, $\mathscr{I}_4$, and J. It is also desirable to test the moment truncation procedure by modifying equation (89d) so as to introduce skewness into the relative velocity distribution.

A large number of models and variations were considered; results of representative cases will be discussed here. Distinguishing features of each model are given in Table 1 and Figures 1–4. Column (5) of the table gives ξ_{MAX} for each model, defined as the value of ξ for which $d \ln \xi/du = -2$ (the value of ξ at the peak of $s^2\xi$). Column (6) gives ξ_{BEND} for each model, defined as the value of ξ where the curve crosses the $s^{-\gamma}$ asymptote. In a two-power-law approximation to our results, ξ_{BEND} would be the approximate point of intersection. The value of Q which yields the correct boundary conditions is given in column (7) of Table 1. A measure of the isotropy of the velocity dispersion at small s is $\langle v_r^2\rangle/\langle v_t^2\rangle$. This is given in column (8). Plotted in Figures 1–3 are the functions $s^2\xi(s)$, $s^2A(s)$, $s\mathbf{\Pi}(s)$ and $s\mathbf{\Sigma}(s)$ for models 1–3. For these figures, $s\mathbf{\Pi}$ and $s\mathbf{\Sigma}$ have been divided by 10 to bring them into the same range as the other functions. Figure 4 compares $s^2\xi(s)$ for all the models. The dotted line is the small s asymptote, $s^{2-1.77}$.

The models are distinguished primarily by the assumed forms of $\mathscr{I}_1$ and $\mathscr{I}_4$. In Table 1, columns (2) and (3) describe whether "algebraic" coupling "A" (i.e., eqs. [93] or [95]) or "differential" coupling "D" (i.e., eq. [94]) is used for the models of $\mathscr{I}_1$ and $\mathscr{I}_4$. Additional models were formed by multiplying $\mathscr{I}_1$ and $\mathscr{I}_4$ by an additional factor $\boldsymbol{F}$, which has the following definitions in the models labeled a, b, and c in Table 1:

$$\begin{aligned} \boldsymbol{F} &= 1 && \text{model a} \\ &= 1 + s/s_0 && \text{model b} \quad (s_0 = 1) \\ &= (1 + s/s_0)^{-1} && \text{model c} \end{aligned} \tag{105}$$

The sixth term and that part of the fifth term of equation (89d) contributed by the $x^\alpha x^\beta x^\gamma/x^3$ component of the third velocity moment (see eq. [57]) have been eliminated in all models except number 3. As explained above, these terms are important only in the transition zone. Elimination of the terms effectively introduces a skewness in the velocity distribution that is relatively large, $\langle(v - \bar{v})^3\rangle/\langle v^3\rangle \approx 1$, at $\xi \approx 1$, but it has only a small effect on the solutions because the divergence of this contribution, which is all that enters equation (89d), is small.

All attempts to model $\mathscr{I}_1$ by equation (91) failed, in the sense that no value of Q yields the wanted behavior at the boundaries. Apparently, in this model, we need another eigenvalue, as well as Q. This model probably fails because, according to equation (91), $\mathscr{I}_1$ has a sign change at $d \ln \xi/d \ln s = -1.5$ and, as seen in Figures 1–4, $s^2\xi$ usually shows a "bump" in the transition region where the logarithmic derivative of ξ is greater than -1.5. Thus two sign changes occur in $\mathscr{I}_1$ in a relatively short interval, and this unphysical behavior yields a solution having peculiar characteristics.

Models 4–7 are variations on model 2 where $\mathscr{I}_1$ and $\mathscr{I}_4$ have been multiplied by the function $\boldsymbol{F}$, which is unity at small s and which varies either as s or as s^{-1} at large s. $\boldsymbol{F}$ is parametrized by a cutoff s_0, and models 4–7 all have $s_0 = 1$, so that $\mathscr{I}_1$ and $\mathscr{I}_4$ are changed a factor of 2 at $\xi \approx 3$ (see Figs. 1–4). Models 4 and 5 increase the strength of $\mathscr{I}_1$ and $\mathscr{I}_4$ and so extend the nonlinear solution, while models 6 and 7 cut off these nonlinear terms faster. There is no physical justification for $\boldsymbol{F}$; it is introduced simply to demonstrate the degree of sensitivity of the models to the method of treating the three-point correlation function in the transition region. As shown in Table 1 and Figure 4, these fairly drastic variations of $\mathscr{I}_1$ and $\mathscr{I}_4$ in the transition zone significantly influence the solution but do not change its basic character—a rather abrupt transition between the two asymptotic solutions.

All solutions shown have been solved with $\boldsymbol{J}(s) = 1$ (eq. [104]), which is accurate within 10% where this term is important. Upon iterating $\boldsymbol{J}(s)$, we find that $\xi(s)$ changes slightly, as does Q, but $\mathbf{\Pi}$ and $\mathbf{\Sigma}$ depart from power law behavior at the large s boundary. We have not studied this problem in detail, because our model for $\boldsymbol{J}(s)$ is significantly wrong only in the transition zone, where $\mathscr{I}_3^{\alpha\beta}$, (eq. [89e]), which we have completely ignored, is of comparable strength, and our models for $\mathscr{I}_1$ and $\mathscr{I}_4$ are uncertain.

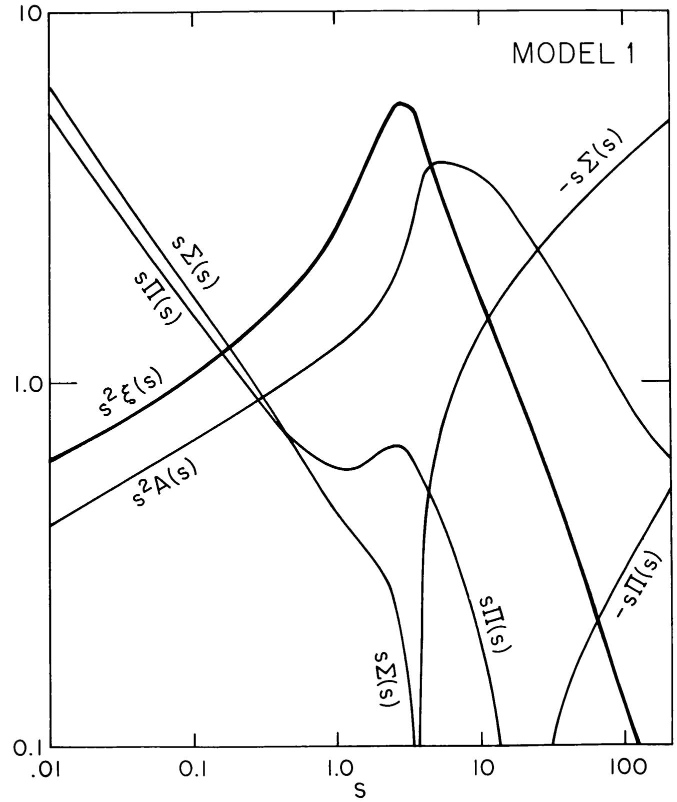

FIG. 1.—Results of the integration for model 1 (see Table 1). The independent variable is the scaled length s (eq. [88]), A measures the mean relative peculiar velocity of particle pairs at fixed separation (eq. [42]), and Π and Σ measure the dispersion of the relative velocity (eq. [51]).

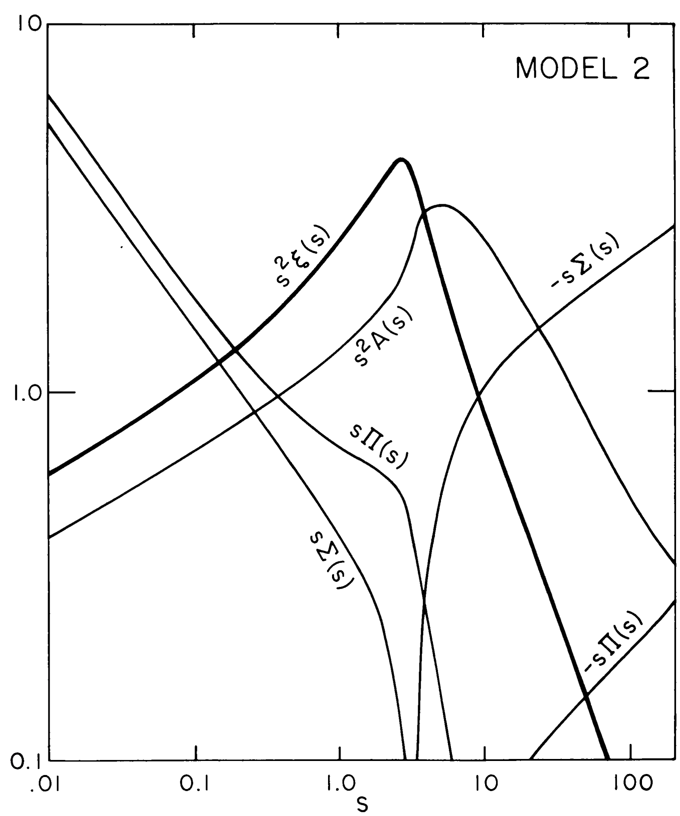

FIG. 2.—Results of the integration for model 2

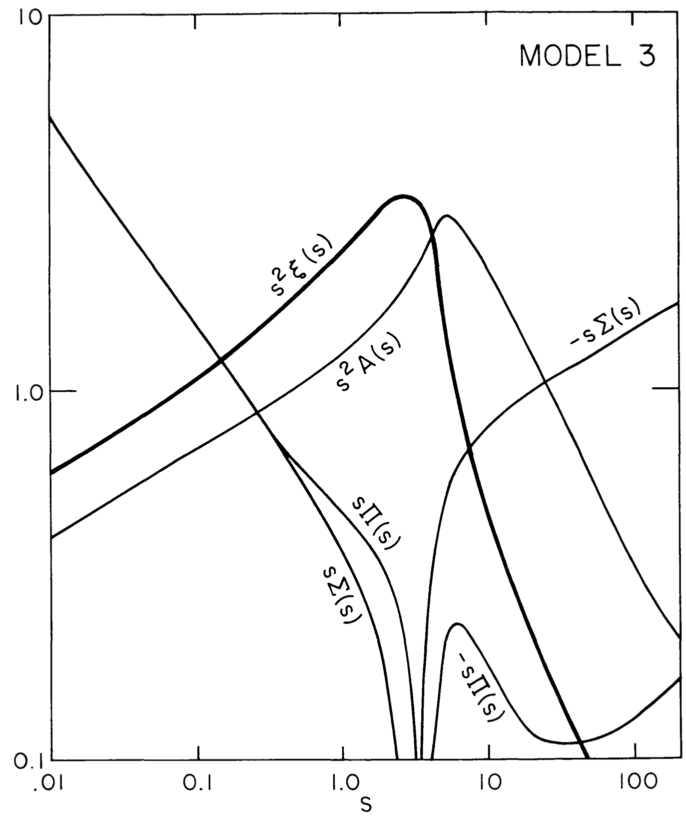

FIG. 3.—Results for model 3, which is the same as model 2 except that all terms are included in eq. (89d)

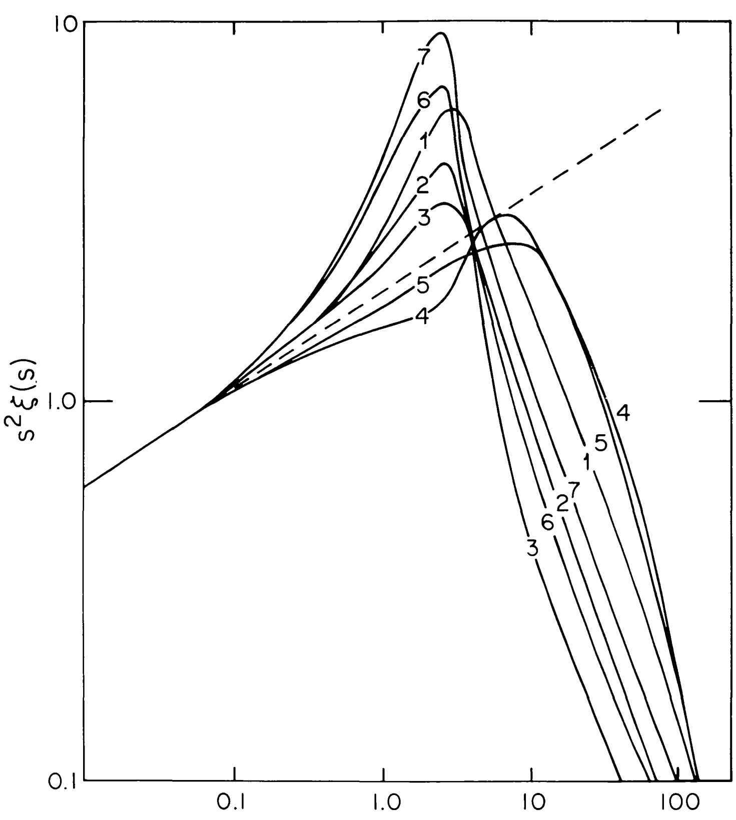

FIG. 4.—The spread of results for the two-point correlation function ξ for different treatments of the transition region. The numbers correspond to the models listed in Table 1. The dotted line is the power law $\xi \propto s^{-1.77}$.

c) *Evaluation of the Velocity Moments*

The velocity moments plotted in Figures 1–3 are converted to physical units by adjusting the length scale so that ξ at small s matches the observed function, $\xi = (r_c/r)^{1.77}$, $r_c \approx 5\,h^{-1}$ Mpc, where the latter number is uncertain by perhaps a factor of 1.5. This gives the conversion factor μ between s and physical lengths measured at the present epoch,

$$r = a_0 x = \mu s\,. \tag{106}$$

Then by equations (52), (53), (80), and (88),

$$\langle v\rangle = \nu A s/(1+\xi)\,,\quad \langle v_1{}^2\rangle = \nu^2 K\,,\quad \langle v_t{}^2\rangle = \nu^2(\boldsymbol{\Sigma} + 2K/3)/(1+\xi)\,,$$
$$\langle v_r{}^2\rangle = \nu^2(\boldsymbol{\Pi} + 2K/3)/(1+\xi)\,. \tag{107}$$

The conversion factor is

$$\nu = 3\mu H/2\,, \tag{108}$$

where H is Hubble's constant. The value of ν is independent of H because r_c and hence μ scales as H^{-1}.

Figure 5 shows the velocity moments converted to kilometers per second and based on the solution in Figure 3. The horizontal line is the single-particle rms peculiar velocity in one dimension, $(\langle v_1{}^2\rangle/3)^{1/2} \approx 625(r_c/5\,h^{-1}$ Mpc) km s^{-1}. It will be noted that the velocity scale ν varies as r_c, so it is uncertain by a factor of about 1.5, and that all the solutions here assume $\Omega \approx 1$. The scale is independent of h because r_c scales as h^{-1}.

XIV. DISCUSSION

a) *The Shape of ξ and the Value of Q*

The central goal of the calculation has been to compute the shape of the two-point correlation function ξ and the value of the parameter Q in the three-point function under the standard gravitational instability picture. This is a difficult problem, so an essential first check is the consistency of results from different methods of attack and, in one method, consistency under changes of details of the approximation. In the present method the main assumptions have been (1) that we can neglect the third central moment of the distribution of relative peculiar velocities

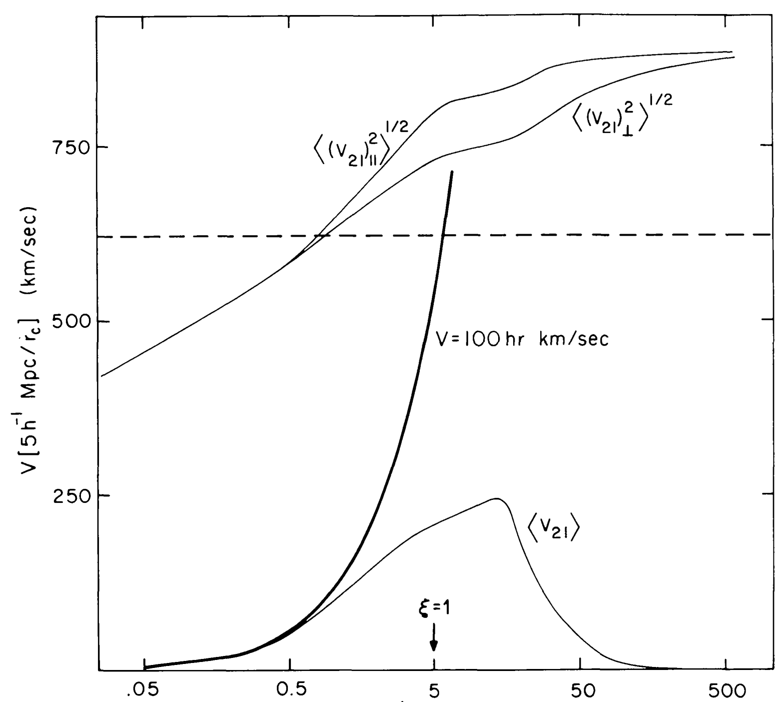

FIG. 5.—Velocity moments. These results are based on model 3 in Table 1. The horizontal line is the rms peculiar velocity in one dimension for randomly chosen particles, $-\langle v_{21}\rangle$ is the mean difference of peculiar velocities for pairs chosen at random, and $\langle (v_{21})_{\parallel}{}^2\rangle$ and $\langle (v_{21})_{\perp}{}^2\rangle$ are the mean square values of the components of the relative peculiar velocity v_{21} along the line joining the particles and along a line at right angles to this. These curves scale with the parameter r_c (eq. [4]) as indicated in labels along the axes. The vertical axis is independent of h; the horizontal axis scales as h^{-1}.

of particle pairs at any separation x, and (2) that the three-point correlation function can be modeled in terms of the two-point function by equations (4) and (62).

The first assumption is the lowest order approximation that can describe galaxy clustering. Although we know that some degree of skewness must be present in the two-point distribution function, it seems unlikely that our results, especially the shape of ξ, are strongly affected by this approximation. In the context of spherical clusters described using a Vlasov equation, van Albada (1960, 1961) has shown that initial irregularities can develop into stable clusters in the absence of kinetic energy flux in the single-particle velocity distribution, and that the essential characteristics of the velocity distribution do not change when skewness is included. Our results have a qualitatively similar behavior.

Comparison of model 2, which has skewness because it neglects several terms in equation (89d), and model 3, which is identical except that it has no skewness, discloses no major differences. This point could be further tested by results from other methods such as N-body models (e.g., Peebles and Groth 1976; Aarseth and Icke 1976). Because the first relative velocity moment is a function of the separation of the particles, there will be skewness in the relative velocity distribution if pairs of all separations are included together.

For the second assumption we must consider several points. In the "main equation" for ξ, equation (50c), we need the spatial three-point function ξ. Observations of ζ for galaxies are quite detailed at $\xi \gg 1$ but extend to a maximum separation of 3°, corresponding to $\sim 10\, h^{-1}$ Mpc, in the Shane-Wirtanen catalog. Thus equation (4) for ζ might be in error in the "transition region" $\xi \approx 1$, where ξ is breaking away from the power law. We have a test of sensitivity of the computations to this because we have modeled the integrals over ζ and d by expressions accurate when $\xi \gg 1$ but only approximate in the transition region. In effect, we have inserted deviations from equation (4) in the transition region, and by using different models we have shown that the results are not very sensitive to these deviations. The second point is that we are assuming that the galaxy correlation functions agree with the mass correlation functions. There is an important piece of evidence in favor of this: ζ is observed to scale as ξ^2, in agreement with what is predicted for the mass functions in the gravitational instability picture (Peebles 1974). The third point is that in the "auxiliary equation" (eq. [50d]) we need a first velocity moment of the three-point space and velocity correlation function d. We have estimated this by using the law of conservation of triplets, which also involves the first moment. Since the combination is not the same in the conservation equation and in equation (50d), there is some ambiguity here, but this may not be too serious because the main equation ought to be somewhat insensitive to errors in this auxiliary equation.

By construction, all solutions for $\boldsymbol{\xi}$ agree at the small s limit. The deviations of the curves in the transition and large s regions (Fig. 4) are some measure of the uncertainty of our predictions. There is a factor of ~ 6 spread in the amplitude of $\boldsymbol{\xi}$ in the large s limit. In most models, the power law index does not simply roll from one asymptotic behavior to the other; rather, going from small s to large s the index first drops below γ (eq. [7]), then rapidly goes above 3, then moves down to the asymptotic value $3 + n$. This behavior occurs for all n we have tried ($-0.9 < n < 0.75$). The rise above the power law $r^{-\gamma}$ usually amounts to less than a factor of 2. This feature, if real, will be difficult to observe.

The break point, $\boldsymbol{\xi}_{\mathrm{BEND}}$, is found to be in the range 0.1–0.25, in all models except models 4 and 5 where $\boldsymbol{\xi}$ is always below the $s^{-\gamma}$ asymptote. In these two models a two-power-law approximation would have a break point at $\boldsymbol{\xi} \approx 0.06$. Prospects for observing the break from the $s^{-\gamma}$ power law are discussed by Davis, Groth, and Peebles (1977).

It is encouraging that the computed values of Q are reasonably close to the measured values, $Q \approx 0.85$ from the Zwicky catalog and $Q \approx 1.24$ from the Shane-Wirtanen catalog (Peebles and Groth 1975; Groth and Peebles 1976). By the arguments of § IIb, Q must be greater than ~ 0.3 to ensure a positive dispersion in the number of particles about a randomly chosen particle, but the equations do not guarantee this physical constraint. Given the degree of approximation in the models, we might have found Q of order 10, or 0.1. The fact that Q is calculated to be of the order of unity is evidence that our modeling of the equations is reasonable.

Comparison of the calculated Q with observations should be made with caution because Q always appears in equation (89) multiplied by M_γ (eq. [92]). Roughly 40% of the integral for M_γ is contributed from the region $s < 0.01$, corresponding to $r \leq 50\, h^{-1}$ kpc today, and we might expect nongravitational forces to have reduced subclustering on scales this size and smaller. Therefore we have overestimated M_γ and correspondingly underestimated Q by a factor of up to 1.7.

b) *The Velocity Dispersion*

The auxiliary functions $\boldsymbol{\Sigma}$ and $\boldsymbol{\Pi}$ are less reliably predicted in our calculation. Comparison of Figures 1–3 shows that the behavior of $\boldsymbol{\Pi}$ in particular varies rather dramatically from model to model in the transition region. This is because $\boldsymbol{\Pi}$ never plays a dominant role in the equations and is able to fluctuate to balance various terms in the different models. The computed ratio of $\boldsymbol{\Pi}$ to $\boldsymbol{\Sigma}$ at small s (Table 1) is quite insensitive to the approximations, and is close to unity, that is, close to isotropy. This is an important test of reasonableness in the sense that strong asymmetry would have seemed unreasonable. The velocity moments plotted in Figure 5 offer some prospects for further observational tests. The computed relative peculiar velocity dispersion $\langle v_{21}{}^2 \rangle$ at $r \lesssim 1\, h^{-1}$ Mpc agrees with the "cosmic virial theorem" derived by Peebles (1976a, b) under the assumption of stability and isotropy

(**Π** = **Σ**). An observational test of at least the magnitude of the dispersion along this part of the curve might be possible from complete samples of redshifts to $m \approx 15$ in selected areas (Peebles 1976*a*, *b*). It would be of considerable interest to test for the predicted break in the dispersion curve at $r \approx 5\,h^{-1}$ Mpc. This will be difficult, however, for a survey to $m \approx 15$ may not be a fair sample on scales much larger than $5\,h^{-1}$ Mpc.

The horizontal line in the figure is the rms peculiar velocity of individual galaxies, about $625(r_c/5\,h^{-1}$ Mpc) km s^{-1} in one dimension, consistent with the estimate of Fall (1975). Observational tests of this number will be difficult because it is much harder to pick out the absolute motion of galaxies (relative to the comoving coordinates of the background homogeneous cosmological model) than to pick out the relative motions of galaxy pairs.

The bottom line in Figure 5 gives the mean relative peculiar velocity $\langle v_{21}\rangle$ averaged over all pairs at separation r. At small r $\langle v_{21}\rangle$ is close to Hr and opposite in sign: consistent with the assumption of stability, the mean rate of proper separation is near zero. At $\xi = 1$, $r \approx 5\,h^{-1}$ Mpc, and $\langle v_{21}\rangle$ is about 40% of the Hubble flow, fairly close to the estimate found in another way by Peebles and Groth [1976, eq. (33)]. Sargent and Turner (1976) have discussed a possible method of measuring $\langle v_{21}\rangle$. Because we cannot tell which of a close galaxy pair is more distant, we can only see the effect of $\langle v_{21}\rangle$ through the width of the distribution of redshift differences for galaxy pairs at chosen angular separation: if $\langle v_{21}\rangle$ is opposite to r_{21} it narrows the distribution. The problem is that **K**, **Π**, and **Σ** broaden the distribution, and it may be difficult to untangle effects.

c) *Virialization and Overshoot of* $\langle v_{21}\rangle$

Gott and Rees (1975) have argued that at $\xi \approx 1$ the $\langle v_{21}\rangle$ curve in Figure 5 ought to rise above the Hubble line Hr. This is based on the assumption that the development of a cluster of particles is adequately described by the homogeneous sphere model. In this model the points in a protocluster all come to rest at the point of maximum expansion at the same time. The cluster must then collapse by a factor of 2 in radius to generate enough internal kinetic energy to satisfy the virial theorem. This collapse would make $|\langle v_{21}\rangle|$ greater than Hr when r is comparable to the typical size of protoclusters that are collapsing. If $\langle v_{21}\rangle$ behaved in this way, then, through equation (41), it would make the shoulder in ξ rise from $\xi \approx 0.25$ as found here up to $\xi \gg 1$ (Gott and Rees 1975). The effect of collapse on $\langle v_{21}\rangle$ when $\xi \leq 1$ is diluted by uncorrelated pairs. However, this collapse effect is questionable because it is doubtful that the spherical model is an adequate approximation for this purpose. For the internal motions of a protocluster near "maximum expansion," a better model would be the pancake picture of Zel'dovich (1976 and earlier references therein). This shows that the protocluster can be collapsing along one axis while it still is expanding in other directions and while the mean density as measured by $\xi(r)$ (that is, the density averaged over a spherical shell) still is decreasing. That is, the protocluster can be "previrialized" due to the development of nonradial motions while it still is expanding as a whole.

A second "previrialization" effect is the production of internal kinetic energy through tidal interaction among neighboring protoclusters. We know that this effect makes the final kinetic energy of rotation of a cluster at least comparable in order of magnitude to the total energy (Peebles 1971*b*). The internal velocity field produced by this tidal interaction tends to have total kinetic energy appreciably greater than the energy associated with the final uniform rotation because the tidal interaction does not produce axisymmetric rotation. Thus it appears that there can be strong previrialization by kinetic energy production through this process. In the model computations it happens that the dispersion functions **Π** and **Σ** at large s increase fast enough with decreasing s that, by the time ξ reaches unity, the dispersion is enough to satisfy the virial theorem. It is difficult to know whether this is because the computation adequately reflects the previrialization effects mentioned above or because the approximations have artificially eliminated the "virialization" effect. The key test will be the comparisons with results from other methods of attacking the problem.

d) *The Next Step*

We emphasize that the results presented here are far from complete because we have assumed $\Omega \approx 1$ (as well as $\Lambda = 0$, pressure negligible). The next substantial step will be to extend the detailed computation to cases where Ω is substantially different from 1 by using the present results as initial values at high redshift. Some estimates of the expected effects of lowering Ω are discussed by Davis, Groth, and Peebles (1977). We hope to report on the results of a detailed computation in due course.

It is a pleasure to acknowledge helpful discussions with M. Geller, M. Krook, M. Lecar, and G. Rybicki. We thank M. Fall for a careful reading of the manuscript. This work commenced while P. J. E. P. enjoyed the hospitality of the physics department at the University of California, Berkeley, in 1974.

REFERENCES

Aarseth, S., and Icke, V. 1976, private communication.
Acton, F. S. 1970, *Numerical Methods that Work* (New York: Harper and Row), p. 481.
Bisnovatyi-Kogan, G. S., and Zel'dovich, Ya. B. 1971, *Soviet Astr.—AJ*, **14**, 758.
Davis, M., Groth, E. J., and Peebles, P. J. E. 1977, *Ap. J.* (*Letters*), **212**, L107.
Fall, S. M. 1975, *M.N.R.A.S.*, **172**, 23p.
Fall, S. M., and Saslaw, W. C. 1976, *Ap. J.*, **204**, 631.
Fall, S. M., and Severne, G. 1976, *M.N.R.A.S.*, **174**, 241.

Gilbert, I. H. 1965, Ph.D. thesis, Harvard University.
———. 1966, *Ap. J.*, **144**, 233.
Gott, J. R., and Rees, M. 1975, *Astr. Ap.*, **45**, 365.
Groth, E. J., and Peebles, P. J. E. 1977, *Ap. J.*, in press.
Henon, M. 1961, *Ann. d'Ap.*, **24**, 369.
Ichimaru, S. 1973, *Basic Principles of Plasma Physics* (Reading, Mass.: Benjamin), p. 300.
Inagaki, S. 1976, *Pub. Astr. Soc. Japan*, **28**, 77.
Irvine, W. M. 1961, Ph.D. thesis, Harvard University.
Larson, R. B. 1970, *M.N.R.A.S.*, **147**, 323.
Layzer, D. 1963, *Ap. J.*, **138**, 174.
Lynden-Bell, D., and Wood, R. 1968, *M.N.R.A.S.*, **138**, 495.
Montgomery, D. C., and Tidman, D. A. 1964, *Plasma Kinetic Theory* (New York: McGraw-Hill), chap. 4.
Peebles, P. J. E. 1965, *Ap. J.*, **142**, 1317.
———. 1971*a*, *Physical Cosmology* (Princeton: Princeton University Press).
Peebles, P. J. E. 1971*b*, *Astr. Ap.*, **11**, 377.
———. 1974, *Ap. J.* (*Letters*), **189**, L51.
———. 1975, unpublished lecture notes.
———. 1976*a*, *Ap. Space Sci.*, **45**, 3.
———. 1976*b*, *Ap. J.* (*Letters*), **205**, L109.
Peebles, P. J. E., and Groth, E. J. 1975, *Ap. J.*, **196**, 1.
———. 1976, *Astr. Ap.*, **53**, 131.
Rice, S. A., and Gray, P. 1965, *The Statistical Theory of Simple Liquids* (New York: Interscience), p. 74.
Sargent, W. L. W., and Turner, E. L. 1976, preprint.
Saslaw, W. C. 1972, *Ap. J.*, **177**, 17.
Totsuji, H., and Ichimaru, S. 1974, *Prog. Theoret. Phys.*, **52**, 42.
van Albada, G. B. 1960, *B.A.N.*, *Bull. Astr. Inst. Netherlands*, **15**, 165.
———. 1961, *Bull. Astr. Inst. Netherlands*, **16**, 172.
Yahil, A. 1976, *Ap. J.* (*Letters*), **204**, L59.
Zel'dovich, Ya. B. 1976, *Comments on Astrophysics*, **6**, 157.

MARC DAVIS: Center for Astrophysics, 60 Garden Street, Cambridge, MA 02138

P. J. E. PEEBLES: Joseph Henry Laboratories, Physics Department, P.O. Box 708, Princeton, NJ 08540